Graduate School ETD Form 9
(Revised 01/14)

PURDUE UNIVERSITY
GRADUATE SCHOOL
Thesis/Dissertation Acceptance

This is to certify that the thesis/dissertation prepared

By Vinay Kumar Shimoga Muddappa

Entitled
Electrochemical Model Based Condition Monitoring of a Li-ion Battery Using Fuzzy Logic

For the degree of Master of Science in Mechanical Engineering

Is approved by the final examining committee:

Sohel Anwar

Tamer Wasfy

Lingxi Li

To the best of my knowledge and as understood by the student in the *Thesis/Dissertation Agreement. Publication Delay, and Certification/Disclaimer (Graduate School Form 32)*, this thesis/dissertation adheres to the provisions of Purdue University's "Policy on Integrity in Research" and the use of copyrighted material.

Sohel Anwar

Approved by Major Professor(s): _____

_____

Approved by: Sohel Anwar 04/16/2014

Head of the Department Graduate Program Date

ELECTROCHEMICAL MODEL BASED CONDITION MONITORING OF A LI-ION BATTERY USING FUZZY LOGIC

A Thesis

Submitted to the Faculty

of

Purdue University

by

Vinay Kumar Shimoga Muddappa

In Partial Fulfillment of the

Requirements for the Degree

of

Master of Science in Mechanical Engineering

May 2014

Purdue University

Indianapolis, Indiana

This thesis is dedicated to my beloved parents, father Muddappa S and mother Rathna. All I have and will accomplish are only possible due to your love and sacrifices. I also dedicate this thesis to my lovely wife, Ramya Vinay, who supported me each step of the way; to my beloved sister, Dr. Vidya SM and brother, Mallikarjuna SM who have been instrumental in my achievements.

ACKNOWLEDGMENTS

I would like to gratefully acknowledge my thesis adviser, Dr. Sohel Anwar for his assistance, guidance, and supervision during the entire course of thesis research and thesis work. Dr. Anwar generously shared with me his research experience and directed me towards perfection in every detail, for which I am always thankful.

I am extremely grateful to my family, colleagues and friends for their support and encouragement.

I would also like to thank my fellow students and friends, Pavan Kumar Reddy, Bibin N Pattel and Amardeep Singh Sidhu for their help and support during this phase of my life. I thank Ms. Valerie Lim Diemer and Mr. Mark Senn for assisting me in formatting this thesis.

TABLE OF CONTENTS

Page

LIST OF TABLES vi

LIST OF FIGURES vii

ABBREVIATIONS viii

ABSTRACT ix

1 Introduction 1

1.1 Overview 1

1.2 Structure of Lithium-ion Batteries 1

1.3 Chemistry of Lithium-ion Batteries 2

1.4 Major Contributions of Thesis Work 4

1.5 Organization of this Thesis 5

2 Literature survey 7

2.1 State Estimation Based Diagnostics 7

2.2 Data Driven Fault Detection and Diagnosis 8

3 Electrochemical battery modeling 10

3.1 Electrochemical Model 10

3.2 Battery Temperature Model 15

3.3 OCP Equation of Electrode Material 15

3.4 Solving Electrochemical Model 16

4 Electrochemical model based observer 19

4.1 Model Reduction 19

4.2 Observer Design 21

4.3 Initial and Boundary Conditions of Observer 23

4.4 Simplified OCP Equation of Electrode Material 24

4.5 Solving Electrochemical Model Based Observer 24

Page

5 Fuzzy Logic Based Condition Diagnosis 30
5.1 Model based FDD 31
5.2 Simulink Design for FDD 32
5.2.1 Membership Functions(MF) 33
5.2.2 Decision Signal Generation 38
6 Design of experiments 40
6.1 Battery Chemistry and Battery Parameter Values 40
6.2 Hybrid Pulse Power Characterization Drive Cycle 42
7 Diagnosis performance evaluation 46
7.1 Fault Injection 46
7.2 Fault Detection 47
8 Conclusion 52
8.1 Conclusion 52
8.2 Recommendation for Future Work 53
LIST OF REFERENCES 55

LIST OF TABLES

Table Page

5.1 Fuzzy rule base for the lithium-ion FDD 39

6.1 LiCoO2 and LiC6 system parameters used for the simulation [34] . . . 41

6.2 Healthy, Degraded, OD and OC battery parameters 43

LIST OF FIGURES

Figure		Page
1.1	Lithium-ion battery structure [5]	3
1.2	Lithium-ion charging and discharging process [6]	3
3.1	Lithium-ion electrochemical battery model [12]	11
3.2	Plant model voltage output C/2, 1C, and 2C discharge rate	17
3.3	Plant model temperature output C/2, 1C, and 2C discharge rate	18
4.1	OCP negative electrode [37]	25
4.2	OCP negative electrode [37]	26
4.3	Voltage output: Observer vs plant model at different gain values	27
4.4	Voltage output: Observer vs plant model at optimal gain value	28
4.5	Temperature output: Observer vs plant model at optimal gain value	29
5.1	Model based fault diagnosis block diagram [39]	31
5.2	Matlab/Simulink design for the FDD	33
5.3	Voltage residual fuzzy MF	34
5.4	Temperature residual fuzzy MF	35
5.5	SOC residual fuzzy membership function	36
5.6	Battery voltage level fuzzy MF	36
5.7	Battery temperature change MF	37
5.8	Battery SOC level fuzzy MF	38
5.9	Fault decision output MF	39
6.1	Complete hybrid pulse power characterization Sequence	44
6.2	Hybrid pulse power characterization profile	45
7.1	Lithium-ion battery plant versus observer outputs	48
7.2	Voltage, temperature and SOC residuals	49
7.3	Voltage, temperature and SOC residuals	50
7.4	Fuzzy output and diagnostics decision	51

ABBREVIATIONS

ARMA	auto regressive moving average
ECM	electrical circuit model
FDD	fault detection and diagnosis
FL	fuzzy logic
HEV	hybrid electric vehicle
HPPC	hybrid pulse power characterization
IS	impedance spectroscopy
MF	membership function
MMAE	multiple model adaptive estimation
NN	neural networks
OCV	open circuit voltage
OCP	open circuit potential
OC	over-charge
OD	over-discharge
PDAE	partial differential algebraic equation
RUL	end of useful life
SEI	solid electrolyte interface
SOC	state of charge
SOH	state of health
SPM	single particle model

ABSTRACT

Shimoga Muddappa, Vinay Kumar. M.S.M.E, Purdue University, May 2014. Electrochemical Model Based Condition Monitoring of a Li-ion Battery Using Fuzzy Logic. Major Professor: Sohel Anwar.

There is a strong urge for advanced diagnosis method, especially in high power battery packs and high energy density cell design applications, such as electric vehicle (EV) and hybrid electric vehicle segment, due to safety concerns. Accurate and robust diagnosis methods are required in order to optimize battery charge utilization and improve EV range. Battery faults cause significant model parameter variation affecting battery internal states and output. This work is focused on developing diagnosis method to reliably detect various faults inside lithium-ion cell using electrochemical model based observer and fuzzy logic algorithm, which is implementable in real-time. The internal states and outputs from battery plant model were compared against those from the electrochemical model based observer to generate the residuals. These residuals and states were further used in a fuzzy logic based residual evaluation algorithm in order to detect the battery faults. Simulation results show that the proposed methodology is able to detect various fault types including overcharge, over-discharge and aged battery quickly and reliably, thus providing an effective and accurate way of diagnosing li-ion battery faults.

1. INTRODUCTION

1.1 Overview

Lithium-ion batteries are family of rechargeable batteries which can provide mainly two functions, one is to store energy in electro-chemistry and other is to provide electric power supply. The two functions are generally called as charging and discharging [1]. They are one of the most efficient solution for storage of renewable energy and mobile solutions due to high electrochemical potential and high energy density. They are the most popular types of batteries in portable consumer electronics and devices. Their highest energy density, high power density, no memory effect and low self-discharge rate when not in use as compared to there alternatives has increasingly driven use of these batteries in automotive and aerospace applications [2]. Along with all these advantages, lithium-ion battery comes with safety concerns. Many failure mechanisms are identified which may lead to abrupt or gradual battery degradation. In some cases these failure conditions may lead to irreparable damage or dangerous failure conditions [3]. Hence there is a need of diagnostics which detect these failure conditions early. Based on these detections appropriate actions can be taken to protect lithium ion battery. In this thesis, a diagnostics method has been developed to reliably detect failures based on the model based diagnostics technique.

1.2 Structure of Lithium-ion Batteries

Electrical battery is a device which can convert chemical energy to electrical energy. A battery consists of a positive electrode, a negative electrode and electrolyte [4]. Mainly there are two types of electrical batteries: Primary batteries, which can only be used once, these are also called as disposable batteries; and secondary batteries,

which can be used multiple times by charging and recharging, these are also called as rechargeable batteries. Lithium-ion battery falls into secondary battery type.

A typical lithium-ion battery has five components namely cathode (positive electrode), anode (negative electrode), electrolyte, separator and package. Figure 1.1 shows the structure of lithium-ion battery in a prismatic type. In this battery, positive electrode and negative electrode are separated by a separator. The separator is a very thin sheet of microperforated plastic which allows ions to pass through. Separator is soaked with non-aqueous electrolyte to connect the two electrodes. Inside the case cathode, anode and separator are submerged in an organic solvent that acts as the electrolyte. An important function of the case or package is to isolate the internal cell from external elements like water or moisture. The lithium-ion battery is highly sensitive to water which can react to lithium metal or electrolyte to breakdown the battery. Gas release vent is also designed into the case to prevent the battery from exploding because of high internal gas pressure created inside the battery during its normal operation [1].

The three participants in the electrochemical reactions in a lithium ion battery are the anode, cathode, and the electrolyte. The cathode is made up of some active materials like $LiCoO_2$, $LiFePO_4$, $LiMn_2O_4$,$LiNiO_2$,$Li(Li_aNi_xMn_yCo_z)O_2$, $LiCo_{1/3}Ni_{1/3}Mn_{1/3}O$ etc. The anode is made up of materials like graphite, hard carbon, ($LiPF_6$), Li_4Ti_5O12, Si, Ge etc. Electrolytes can be in liquid or solid form. Liquid electolytes contain lithium salts, such as $LiPF_6$, $LiBF_4$ or $LiClO_4$ in an organic solvent, such as ethylene carbonate, diethyl carbonate and dimethyl carbonate [1]

1.3 Chemistry of Lithium-ion Batteries

As a secondary battery type, the lithium-ion battery works in charging and discharge process. Lithium-ions can move in and out of both positive and negative electrodes.The process of lithium-ions moving into the electrode is referred as intercalation and process of lithium-ion moving out of the electrode is referred as deintercalation.

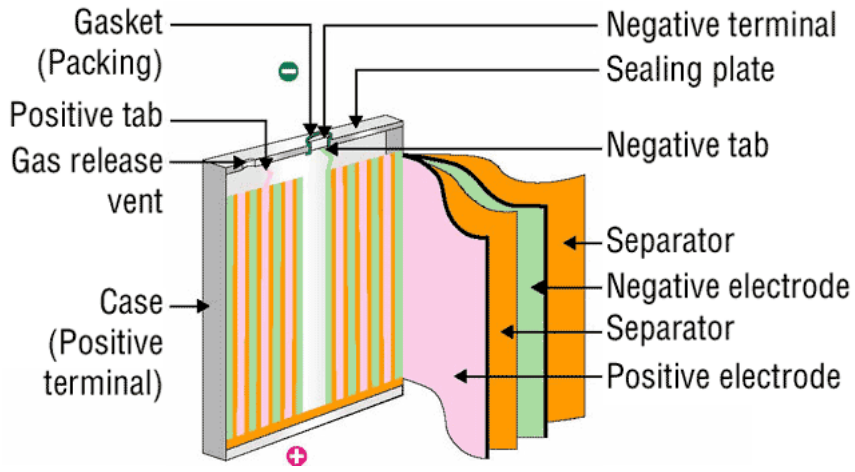

Fig. 1.1. Lithium-ion battery structure [5]

During charging process, the lithium-ions move from positive electrode through electrolyte and are inserted to negative electrode, where they become embedded in the porous electrode material. During discharge process, lithium ions are extracted from negative electrode and moved to the positive electrode through electrolyte. Charging and discharging process is shown in Figure 1.2.

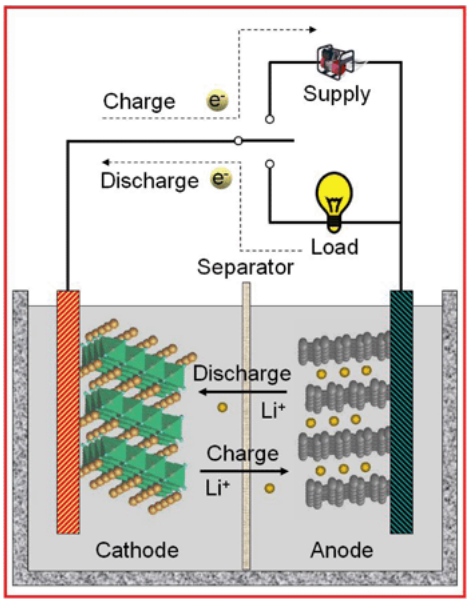

Fig. 1.2. Lithium-ion charging and discharging process [6]

Let us take an example of battery chemistry where in anode is made up of $LiCoO_2$ and cathode is made up of carbon. Electrochemical reaction for this battery chemistry in cathode part is:

$$LiCoO_2 \rightleftharpoons Li_{(1-x)}CoO_2 + xLi^+ + xe^- \tag{1.1}$$

The corresponding electrochemical reaction on anode part is:

$$xLi + + xe^- + 6C \rightleftharpoons Li_xC_6 \tag{1.2}$$

There are some cases where reaction can vary from these standard reactions. For example, in cases where in lithium-ion battery is over-charged and over-discharged. These reactions are irreversible in nature and can lead to defective electrode materials. In over-discharge case, reaction which may happen on cathode side is:

$$Li_+ + LiCoO_2 \rightarrow Li_2O + CoO \tag{1.3}$$

In this reaction, a lithium-ion gets blocked and can never be re-utilized. Also, this reaction destroys cathode material resulting in reduced life of the battery [7]. In over-charge case, reaction which may happen on anode side is:

$$LiCoO_2 \rightarrow Li^+ + CoO_2 \tag{1.4}$$

Similar to the irreversible reaction on cathode this reaction can also cause defect in the active material on cathode to reduce life of the lithium ion battery [8]. Above this, over-charge and over-discharge reactions are exothermic than the normal reactions. They accelerate temperature rise of the battery which may result in thermal runway of lithium-ion batteries.

1.4 Major Contributions of Thesis Work

Main focus of this thesis work is to monitor the lithium-ion battery condition, fault detection and diagnosis. The contribution of this thesis work consists of two parts: First, generation of the residual which can be used by the model based diagnostics

method to monitor battery condition and to detect the fault. Second, developing fuzzy rule based battery condition monitoring and fault detection system.

Generation of the residual is an important process in designing a model based diagnostics method. An electrochemical model based observer was used to generate the residuals. This process also involved fine tuning of the observer gains to accurately track the battery state variables. This observer is computationally less expensive, accurate and efficient to be used for real-time residual generation.

A fuzzy logic based decision logic was developed. This decision logic used residuals of battery output voltage, temperature and SOC along with temperature change, voltage level and SOC level as inputs to monitor battery health and detect the failures.

A plant model capturing all the electrochemical reaction dynamics of the battery, including temperature effects was built. This plant model was used to verify and validate model based fault diagnosis system.

1.5 Organization of this Thesis

Electrochemical based model capturing all battery dynamics along with temperature effect was explored to build plant model in this research. The electrochemcial modeling approach and models are explained in Chapter 2. This is followed by detailed explanation of electrochemical observer based battery model for the observer design and tuning of the observer gains in Chapter 3.

The fault detection technique has two main parts, first part deals with implementation of the observer to generate the residuals, while the second part implements fuzzy logic residual evaluation process. This technique is detailed in Chapter 4.

In Chapter 5, experiments are designed for lithium-ion battery aging, over-charge and over-discharge fault detection, and fault detector was simulated and validated. The simulation results confirm the effectiveness of the fault detection technique. To conclude, Chapter 6 summarizes the details of the fault detection technique in ad-

vantages and drawbacks based on the results of validation. The conclusion is drawn and the possible future scope of work is discussed as well.

2. LITERATURE SURVEY

The fault detection and diagnosis on lithium-ion battery is not young, a lot of work in this area has already been done by researchers. The work on lithium-ion battery fault detection is primarily based on state estimation techniques and empirical techniques or data driven methods.

2.1 State Estimation Based Diagnostics

State estimation based diagnosis encompasses the evaluation of different states of the battery. The choice of the state variables to be estimated mainly be subjected to model of the system being evaluated. For lithium-ion battery open circuit voltage (OCV) and state of charge (SOC) are natural candidates among others. The choice of techniques to evaluate state estimation like standard observers, Luenberger observers (LO), Kalman filter and particle filters differ based on the requirements. The main goal is to access the information of the lithium-ion battery which is not readily obtainable through direct measurements [9]. Luenberger observer based FDD can be found in [10]. Here Chen et al. used bank of reduced order observers on a string of lithium-ion batteries to implement the diagnosis. This approach will work best for the systems with slight or no measurement noise. But it will face inherent difficulties and performance issues in presence of noise. Application of Kalman filter for fault diagnosis can be found in [11]. Here optimal Kalman filtering shows sturdy robustness to noise. Because of adaptive nature of this approach, accurate fault detection is possible.

Lately, multiple state estimation approaches have been proposed using physics based electrochemical model [12]; lumped version of the electrochemical model, usually referred to as single particle model (SPM) [13, 14] and the linearized versions

of the electrochemical model [15, 16]. Success of SPM model and the linearized versions of the electrochemical model are limited to battery operating regime. Their approximations fail in case of high power and high current applications like automotive and aerospace. Electrochemical model captures all the dynamics including the temperature effect, which affects the battery performance intensely. In this work state estimation using electrochemical model presented in [12] was incorporated to design a reliable FDD technique.

2.2 Data Driven Fault Detection and Diagnosis

Extensive study has done on data driven fault detection and diagnosis methods by many researchers. They are based on analysis of time series data. Saha et al [17–19] has done substantial work on this. Nuhic et al. [20] and Wang et al. [21] presented estimation of remaining useful life (RUL) and state of health (SOH) using support vector machine algorithm. This method comprises the application of regression and classification algorithms found under the paradigm of machine learning. Kozlowski et al. [22] proposed parameter identification, estimation and battery prognosis using techniques like impedance spectroscopy (IS), fuzzy logic (FL), neural network (NN) and auto regressive moving average (ARMA). Data driven methods do not truly represent physics behind the modeled process as they are based on objective information, they just capture the relationship between input and output of modeled process. The main hurdle of data driven methods are they need substantial data for their training and have wider confidence intervals as compared to physics based approaches [23]. Further, time involved in training these methods is a concern.

Xiong et al. discussed combination of probability and rule based signal monitoring based lithium-ion battery fault diagnosis and detection [24]. These methods profoundly rely on the thermal signatures of the battery. These thermal signatures in turn depend on the charge and discharge duty cycle applied on the battery. Rocher et al. [25] explained approach to prognosis using model based approach. Here they

analyzed open circuit voltage (OCV) to detect the cell capacity fade due to usage. This approach is worthy for offline applications where in the battery and load can be disconnected for sufficient amount of time to measure the accurate OCV. But, they cannot be used in battery applications like automotive and aeronautical industry. Amardeep et al. [11] demonstrated fault detection and diagnosis using electrical circuit model (ECM) and Multiple Model Adaptive Estimation (MMAE). This approach is ideal if all the fault conditions are known before. This approach fails to detect the unknown fault conditions.

3. ELECTROCHEMICAL BATTERY MODELING

Model for lithium-ion battery can be developed using different techniques namely empirical, neural networks, equivalent circuit and electrochemical or physics based models [2,26,27]. These models vary broadly in terms of computational requirements, complexity and accuracy of their predictions. Empirical modeling techniques capture very less dynamics of the battery making them less efficient in terms of battery state prediction when the operating rage varies broadly. Electrochemical model being physics based mathematical model, predict states of battery with high precision. Hence they are used in this thesis for better, accurate and reliable lithium-ion battery fault detection and diagnosis.

3.1 Electrochemical Model

Electrochemical model is physics-based and is constructed based on electochemical principles. 1D-spatial model, also known as pseudo-two-dimensional model of lithium-ion battery is considered in this thesis. 1D-spatial model considers battery dynamics only in one axis i.e. X-axis neglecting the dynamics along other two axes, Y-axis and Z-axis [28–32]. This model is applicable to cell structures with out-sized cross-sectional area and low currents. A typical lithium-ion battery cell has X-axis length in scale of 100μ, whereas Y-axis and Z-axis length in scale of $100{,}000\mu$ [2].

Figure 3.1 shows the representation of different domains of battery model namely, negative electrode, separator and positive electrode. Positive electrode is made up of very pure metal oxides. Performance and life of battery is directly related to uniformity of metal oxide chemical composition. Negative electrode is made up of layered structure of graphite, a form of carbon. Active materials of both electrode is represented as a continuum of spheres in the model. Positive and negative electrodes

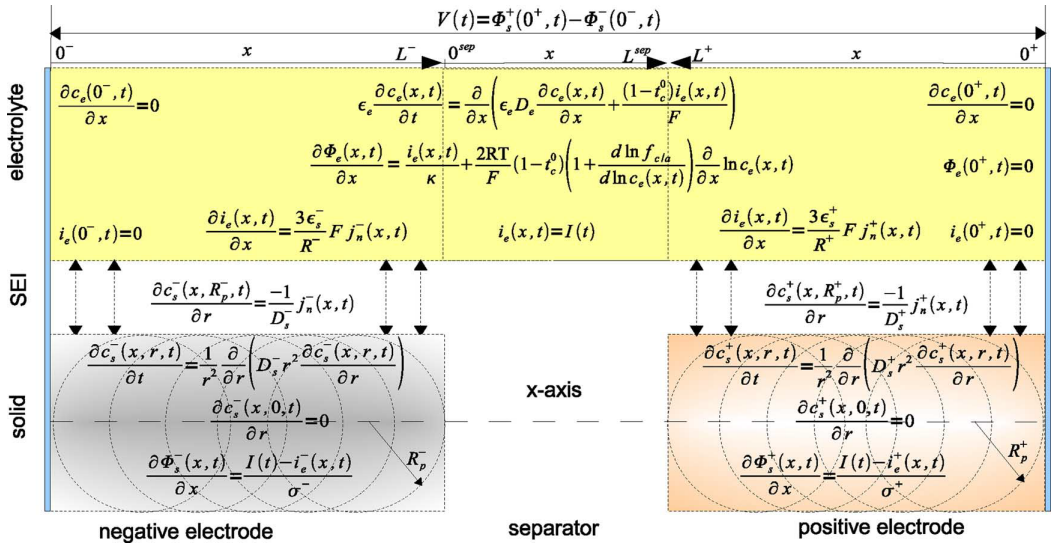

Fig. 3.1. Lithium-ion electrochemical battery model [12]

are separated by a very thin membrane made up of insulating material, but it has property of permeability through which tiny lithium-ions can diffuse. Current through the electrodes is carried by both lithium-ions and electrons, where are in separates current is carried only by lithium-ions. Lithium-ions inside the active material of electrodes and the electrolyte are interconnected through an interface called solid-electrolyte-interface (SEI) by lithium-ion flux [12]. Potential difference between the electrodes is output of the model which is voltage.

At any at any position x, at any time t, the state variables needed to describe the electrochemical model are the lithium ion concentration $c_e(x,t)$ in the electrolyte, the lithium concentration $c_s(r,x,t)$ in the positive and negative electrode, the current $i_s(x,t)$ in the solid electrode, the current $i_e(x,t)$ in the electrolyte, the electric potential $\phi_s(x,t)$ in the solid electrode, the electric potential $\phi_e(x,t)$ in the electrolyte and the molar flux $j_n(x,t)$ of lithium at the surface of the spherical particle [12].

The governing equations for the positive electrode of lithium-ion battery are given by [12, 29, 33].

$$\epsilon_e \frac{\partial c_e(x,t)}{\partial t} = \frac{\partial}{\partial t}(\epsilon_e D_e \frac{\partial c_e(x,t)}{\partial x} + \frac{1-t_c^o}{F} i_e(x,t)) \tag{3.1}$$

$$\frac{\partial c_{s,i}(x,r,t)}{\partial t} = \frac{1}{r^2}\frac{\partial}{\partial r}(D_{s,i}r^2\frac{\partial c_{s,i}(x,r,t)}{\partial r}) \tag{3.2}$$

$$\frac{\partial \phi_e(x,t)}{\partial x} = -\frac{i_e(x,t)}{\kappa} + \frac{2RT}{F}(1-t_c^0)\times(1+\frac{dlnf_{c/a}}{dlnc_e(x,t)})\frac{\partial lnc_e(x,t)}{\partial x} \tag{3.3}$$

$$\frac{\partial \phi_s(x,t)}{\partial x} = \frac{i_e(x,t)-I(t)}{\sigma} \tag{3.4}$$

$$\frac{\partial i_e(x,t)}{\partial x} = \sum_{i=1}^{n}\frac{3\epsilon_s, i}{R_{p,i}}Fj_{n,i}(x,t) \tag{3.5}$$

$$j_{n,i}(x,t) = \frac{i_{0,i}(x,t)}{F}(e^{\alpha_a F\eta_i(x,t)/RT} - e^{\alpha_c F\eta_i(x,t)/RT}) \tag{3.6}$$

where,

$i_{0,i}(x,t)$ is the current density of the main reaction

$\eta_i(x,t)$ is the over-potential of the main reaction

$i_{0,i}(x,t)$ and $\eta_i(x,t)$ are modeled as:

$$i_{0,i}(x,t) = r_{eff,i}c_e(x,t)^{\alpha_a}(c_{s,i}^{max} - c_{ss,i}(x,t))^{\alpha_a}c_{ss,i}(x,t)^{\alpha_c} \tag{3.7}$$

$$\eta_i(x,t) = \phi_s(x,t) - \phi_e(x,t) - U(c_{ss,i}(x,t)) - FR_{f,i}j_{n,i}(x,t) \tag{3.8}$$

where,

$c_{ss,i}(x,t)$ is the ith solid phase concentration

$U_i(c_{ss,i}(x,t))$ is the open-circuit potential of the ith active material in the solid electrode

$c_{s,i}^{max}$ is the maximum possible concentration in the solid phase of the ith active material.

Additionally, r_{eff}, $R_{f,i}$ and $D_{s,i}$ are temperature dependent parameters. The relationship between these parameters and temperature are given by Arrhenius equation. Arrhenius equations for temperature dependency is given by,

$$\Theta(T) = \Theta_{T_0}e^{A_\theta}((T(t)-T_0)/(T(t)T_0)) \tag{3.9}$$

where,

T_0 is a reference temperature

A_θ is a constant

Further, Subramanian et al. [34] developed approximated model for the Equation 3.2 which stands for mass transfer in the solid material. The approximation has been done in the radial direction.

Approximated model is given by,

$$\frac{\partial}{\partial t}\overline{c}_s(x,t) = -\frac{3}{R_p}j_n(x,t), \tag{3.10}$$

$$\frac{\partial}{\partial t}\overline{q}_s(x,t) = -\frac{30D_s}{R_p^2}\overline{q}_s(x,t) - \frac{45}{2R_p^2}j_n(x,t) \tag{3.11}$$

$$c_{ss}(x,t) = \overline{c}_s(x,t) + \frac{8R_p}{35}\overline{q}_s(x,t) - \frac{R_p}{35D_s}j_n(x,t) \tag{3.12}$$

where,

$\overline{c}_s(x,t)$ is volume averaged concentration

$\overline{q}_s(x,t)$ is averaged concentration flux

$c_{ss}(x,t)$ is particle surface concentration

In the above equations ρ_{avg}, R, $R_{p,i}$, α_a, α_c, σ, c_p, h_{cell}, t_c^0, ϵ_e, ϵ_s, r are model parameters and are constant in each region. κ, D_e, $f_{c/a}$ are functions of electrolyte concentration and temperature [35].

Considering this approximation, model for each electrode of lithium-ion battery is given by

(a) Positive electrode, where $x \in [0^+, L^+]$

$$\frac{\partial}{\partial t}\overline{c}_s^+(x,t) = -\frac{3}{R_{p,i}^+}j_n^+(x,t), \tag{3.13}$$

$$\frac{\partial}{\partial t}\overline{q}_s^+(x,t) = -\frac{30D_s^+}{(R_{p,i}^+)^2}\overline{q}_s^+(x,t) - \frac{45}{2(R_{p,i}^+)^2}j_n^+(x,t) \tag{3.14}$$

$$c_{ss}^{+}(x,t) = \overline{c}_{s}^{+}(x,t) + \frac{8R_{p,i}^{+}}{35}\overline{q}_{s}^{+}(x,t) - \frac{R_{p,i}^{+}}{35D_{s}^{+}}j_{n}^{+}(x,t) \tag{3.15}$$

$$\frac{\partial \phi_{e}^{+}(x,t)}{\partial x} = -\frac{i_{e}^{+}(x,t)}{\kappa^{+}} + \frac{2RT}{F}(1-t_{c}^{0}) \times (1 + \frac{dlnf_{c/a}}{dlnc_{e}(x,t)})\frac{\partial lnc_{e}(x,t)}{\partial x} \tag{3.16}$$

$$\frac{\partial \phi_{s}^{+}(x,t)}{\partial x} = \frac{i_{e}^{+}(x,t) - I(t)}{\sigma^{+}} \tag{3.17}$$

$$\frac{\partial i_{e}^{+}(x,t)}{\partial x} = \sum_{i=1}^{n} \frac{3\epsilon_{s,i}^{+}}{R_{p,i}^{+}} F j_{n,i}^{+}(x,t) \tag{3.18}$$

$$j_{n,i}^{+}(x,t) = \frac{i_{0,i}^{+}(x,t)}{F}(e^{\alpha_{a}F\eta_{i}^{+}(x,t)/RT} - e^{\alpha_{c}F\eta_{i}^{+}(x,t)/RT}) \tag{3.19}$$

(b) Negative electrode, where $x \in [0^{-}, L^{-}]$

$$\frac{\partial}{\partial t}\overline{c}_{s}^{-}(x,t) = -\frac{3}{R_{p,i}^{-}} j_{n}^{-}(x,t), \tag{3.20}$$

$$\frac{\partial}{\partial t}\overline{q}_{s}^{-}(x,t) = -\frac{30D_{s}^{-}}{(R_{p,i}^{-})^{2}}\overline{q}_{s}^{-}(x,t) - \frac{45}{2(R_{p,i}^{-})^{2}} j_{n}^{-}(x,t) \tag{3.21}$$

$$c_{ss}^{-}(x,t) = \overline{c}_{s}^{-}(x,t) + \frac{8R_{p,i}^{-}}{35}\overline{q}_{s}^{-}(x,t) - \frac{R_{p,i}^{-}}{35D_{s}^{-}} j_{n}^{-}(x,t) \tag{3.22}$$

$$\frac{\partial \phi_{e}^{-}(x,t)}{\partial x} = -\frac{i_{e}^{-}(x,t)}{\kappa^{-}} + \frac{2RT}{F}(1-t_{c}^{0}) \times (1 + \frac{dlnf_{c/a}}{dlnc_{e}(x,t)})\frac{\partial lnc_{e}(x,t)}{\partial x} \tag{3.23}$$

$$\frac{\partial \phi_{s}^{-}(x,t)}{\partial x} = \frac{i_{e}^{-}(x,t) - I(t)}{\sigma^{-}} \tag{3.24}$$

$$\frac{\partial i_{e}^{-}(x,t)}{\partial x} = \sum_{i=1}^{n} \frac{3\epsilon_{s,i}^{-}}{R_{p,i}^{-}} F j_{n,i}^{-}(x,t) \tag{3.25}$$

$$j_{n,i}^{-}(x,t) = \frac{i_{0,i}^{-}(x,t)}{F}(e^{\alpha_{a}F\eta_{i}^{-}(x,t)/RT} - e^{\alpha_{c}F\eta_{i}^{-}(x,t)/RT}) \tag{3.26}$$

Output voltage of the model is given by,

$$V(t) = \phi_{s}^{+}(0^{+},t) - \phi_{s}^{-}(0^{-},t) \tag{3.27}$$

3.2 Battery Temperature Model

The lumped temperature of the battery is modeled by,

$$\rho^{avg} c_p \frac{dT(t)}{dt} = h_{cell}(T_{amb}(t) - T(t)) + I(t)V(t) - \sum_{(i=1)}^{n} [\int_{0^+}^{0^-} \frac{3\epsilon_{s,i}}{Rp,i} Fjn,i(x,t)\Delta U_i(x,t)dx] \tag{3.28}$$

where,

$$\Delta U_i(x,t) \triangleq U_i(\overline{c}_s, i)(x,t)) - T(t)\frac{\partial U_i(c_{s,i}(x,t))}{\partial T} \tag{3.29}$$

$T_{amb}(t)$ is the ambient temperature

$\overline{c}_{s,i}(x,t)$ is volume averaged concentration of a particle in solid phase

$\overline{c}_{s,i}(x,t)$ is defined as

$$\overline{c}_{s,i}(x,t) = \frac{3}{R_{p,i}^3} \int_0^{R_{p,i}} r^2 c_{s,i}(x,r,t)dr \tag{3.30}$$

3.3 OCP Equation of Electrode Material

The open circuit potential of electrode material is a function of SOC. For $LiCoO_2$(positive electrode) and LiC_6 (negative electrode) battery system which is the subject of this thesis is given by [34],

Positive electrode OCP:

$$U_p = \frac{-4.656 + 88.669\ \theta_p^2 - 401.119\ \theta_p^4 + 342.909\ \theta_p^6 - 462.471\ \theta_p^8 + 433.434\ \theta_p^{10}}{1.0 + 18.933\ \theta_p^2 - 79.532\ \theta_p^4 + 37.311\ \theta_p^6 - 73.083\ \theta_p^8 + 95.96\ \theta_p^{10}} \tag{3.31}$$

where

$$\theta_p = \frac{c_{ss,p}}{c_{s,p,max}} \tag{3.32}$$

Negative electrode OCP:

$$\begin{aligned} U_n = {} & 0.7222 + 0.1387\ \theta_n + 0.029\ \theta_n^{0.5} - \frac{0.0172}{\theta_n} + \frac{0.0019}{\theta_n^{1.5}} \\ & + 0.2808\exp(0.90 - 15\ \theta_n) - 0.7984\exp(0.4465\ \theta_n - 0.4108) \end{aligned} \tag{3.33}$$

where

$$\theta_n = \frac{c_{ss,n}}{c_{s,n,max}} \tag{3.34}$$

3.4 Solving Electrochemical Model

The complex PDAE described above were solved using Modelica. Modelica is a modeling language for component oriented modeling of complex systems like hydraulic, thermal, electrochemical models etc.

The parameter values for $LiCoO_2$ and LiC_6 battery system which was the subject for this thesis work were chosen from [36] and are listed in Table 6.1. Figure 3.2 gives the discharge curves for 1C (30 A/m^2), 2C and 0.5C rates of galvanostatic discharge. Figure 3.3 shows the average internal temperature of the battery during different discharge rates.

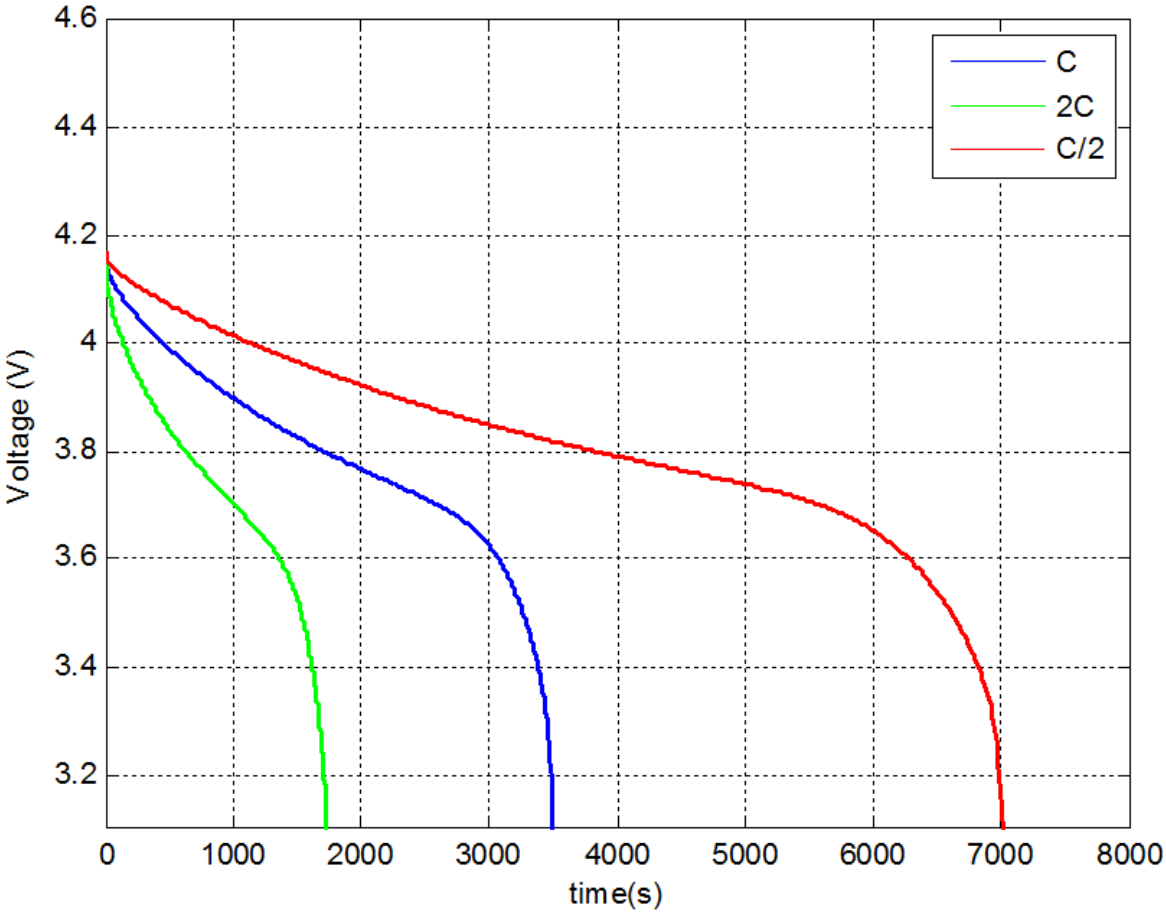

Fig. 3.2. Plant model voltage output C/2, 1C, and 2C discharge rate

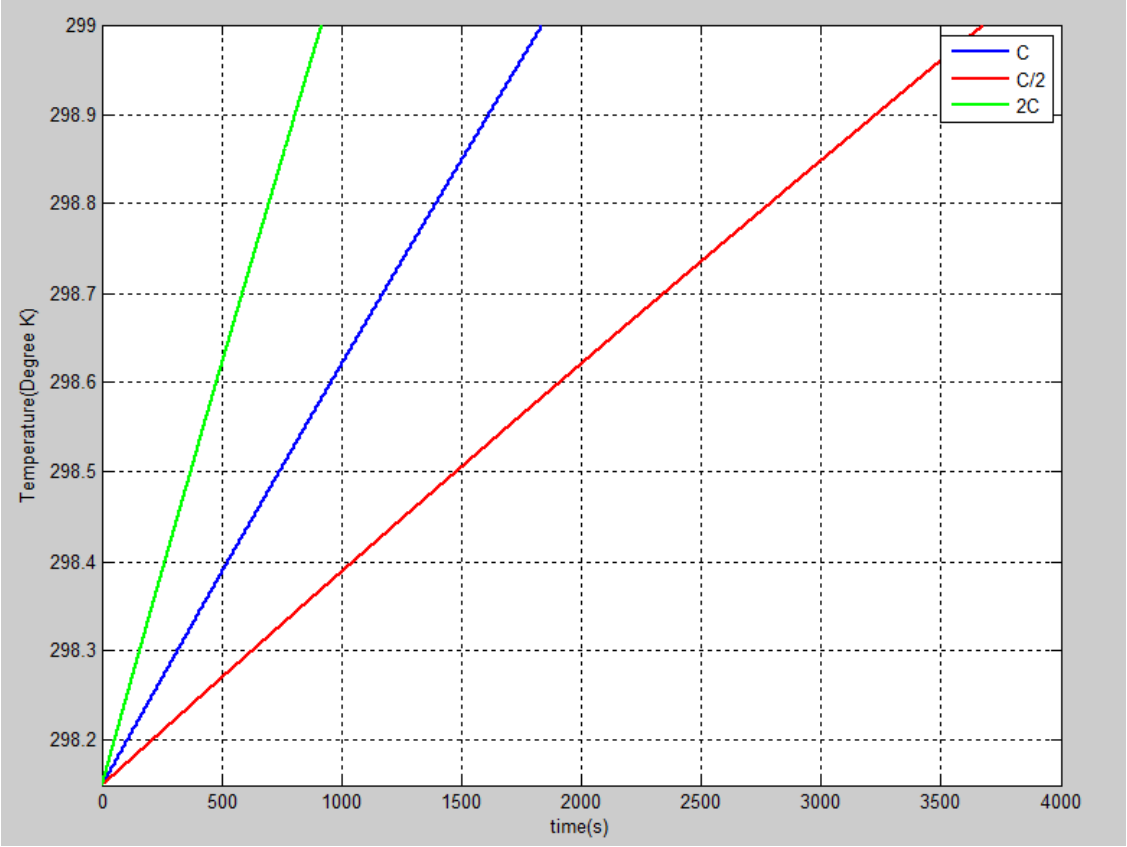

Fig. 3.3. Plant model temperature output C/2, 1C, and 2C discharge rate

4. ELECTROCHEMICAL MODEL BASED OBSERVER

The partial differential algebraic equations (PDAE) model described in Chapter 3 is very complex for model based diagnostics development. They are computationally very expensive, thus limiting usage of this model in real-time applications. There is a different version of approximated PDAE model available in the literature namely single particle model (SPM). This model provide very less information on different states of the battery with reduced accuracy. Additionally, this is not valid if battery has a wide operating range [2].

4.1 Model Reduction

Klein et al, [12] designed an effective approximated model with a key assumption that electrolyte concentration remains constant in battery i.e. $c_e(x,t) = 0$. This simplifies the Equation 3.3 to

$$\frac{\partial \phi_e(x,t)}{\partial x} = -\frac{i_e(x,t)}{\kappa} \tag{4.1}$$

$\because$ since $c_e(x,t) = constant$,

$$\frac{\partial ln c_e(x,t)}{\partial x} = 0$$

therefore,

$$\frac{2RT}{F}(1-t_c^0) \times (1 + \frac{dlnf_{c/a}}{dlnc_e(x,t)})\frac{\partial lnc_e(x,t)}{\partial x} = 0$$

Similarly, Equation 3.1 vanishes as partial derivative of $c_e(x,t) = 0$

This drastically reduces the complexity of the model, thus making it more computationally inexpensive.

Rewriting the approximated model for each electrode,

(a) Positive electrode, where $x \in [0^+, L^+]$

$$\frac{\partial}{\partial t}\overline{c}_s^+(x,t) = -\frac{3}{R_{p,i}^+} j_n^+(x,t), \tag{4.2}$$

$$\frac{\partial}{\partial t}\overline{q}_s^+(x,t) = -\frac{30D_s^+}{(R_{p,i}^+)^2}\overline{q}_s^+(x,t) - \frac{45}{2(R_{p,i}^+)^2} j_n^+(x,t) \tag{4.3}$$

$$c_{ss}^+(x,t) = \overline{c}_s^+(x,t) + \frac{8R_{p,i}^+}{35}\overline{q}_s^+(x,t) - \frac{R_{p,i}^+}{35D_s^+} j_n^+(x,t) \tag{4.4}$$

$$\frac{\partial \phi_e^+(x,t)}{\partial x} = -\frac{i_e^+(x,t)}{\kappa^+} \tag{4.5}$$

$$\frac{\partial \phi_s^+(x,t)}{\partial x} = \frac{i_e^+(x,t) - I(t)}{\sigma^+} \tag{4.6}$$

$$\frac{\partial i_e^+(x,t)}{\partial x} = \sum_{i=1}^{n} \frac{3\epsilon_{s,i}^+}{R_{p,i}^+} F j_{n,i}^+(x,t) \tag{4.7}$$

$$j_{n,i}^+(x,t) = \frac{i_{0,i}^+(x,t)}{F}(e^{\alpha_a F \eta_i^+(x,t)/RT} - e^{\alpha_c F \eta_i^+(x,t)/RT}) \tag{4.8}$$

(b) Negative electrode, where $x \in [0^-, L^-]$

$$\frac{\partial}{\partial t}\overline{c}_s^-(x,t) = -\frac{3}{R_{p,i}^-} j_n^-(x,t), \tag{4.9}$$

$$\frac{\partial}{\partial t}\overline{q}_s^-(x,t) = -\frac{30D_s^-}{(R_{p,i}^-)^2}\overline{q}_s^-(x,t) - \frac{45}{2(R_{p,i}^-)^2} j_n^-(x,t) \tag{4.10}$$

$$c_{ss}^-(x,t) = \overline{c}_s^-(x,t) + \frac{8R_{p,i}^-}{35}\overline{q}_s^-(x,t) - \frac{R_{p,i}^-}{35D_s^-} j_n^-(x,t) \tag{4.11}$$

$$\frac{\partial \phi_e^-(x,t)}{\partial x} = -\frac{i_e^-(x,t)}{\kappa^-} \tag{4.12}$$

$$\frac{\partial \phi_s^-(x,t)}{\partial x} = \frac{i_e^-(x,t) - I(t)}{\sigma^-} \tag{4.13}$$

$$\frac{\partial i_e^-(x,t)}{\partial x} = \sum_{i=1}^{n} \frac{3\epsilon_{s,i}^-}{R_{p,i}^-} F j_{n,i}^-(x,t) \tag{4.14}$$

$$j^{-}_{n,i}(x,t) = \frac{i^{-}_{0,i}(x,t)}{F}(e^{\alpha_a F\eta^{-}_i(x,t)/RT} - e^{\alpha_c F\eta^{-}_i(x,t)/RT}) \tag{4.15}$$

(c) Internal lumped temperature model of battery is given by

$$\begin{aligned}\rho^{avg}c_p\frac{dT(t)}{dt} &= h_{cell}(T_{amb}(t) - T(t)) + I(t)V(t) \\ &- \sum_{(i=1)}^{n^-}[\int_{0^-}^{L^-}\frac{3\epsilon^{-}_{s,i}}{R^{-}_{p,i}}Fj^{-}_{n,i}(x,t)\Delta U^{-}_i(x,t)dx] \\ &- \sum_{(i=1)}^{n^-}+[\int_{0^+}^{L^+}\frac{3\epsilon^{-}_{s,i}}{R^{+}_{p,i}}Fj^{+}_{n,i}(x,t)\Delta U^{+}_i(x,t)dx]\end{aligned} \tag{4.16}$$

Output voltage of the model is given by,

$$V(t) = \phi^{+}_s(0^+,t) - \phi^{-}_s(0^-,t) \tag{4.17}$$

4.2 Observer Design

Afore mentioned approximated model has accuracy issues when the input current to battery is high. In [12] Klein et al. also designed an observer to overcome this issue. They propose observer wherein they take feedback of error between the calculated and the measured voltage and inject it as a linear corrective term in volume averaged concentrations in the individual electrodes. Similarly for the cell temperature, they propose to take feedback of error between calculated and the measure temperature and inject it to internal average temperature model.

Observer equations are given by [12],

(a) Positive electrode, where $x \in [0^+, L^+]$

$$\frac{\partial}{\partial t}\hat{\bar{c}_s}^{+}(x,t) = -\frac{3}{R^{+}_{p,i}}\hat{j}^{+}_n(x,t) + \gamma^{+}_i(V(t) - \hat{V}(t)) \tag{4.18}$$

$$\frac{\partial}{\partial t}\hat{\bar{q}_s}^{+}(x,t) = -\frac{30D^{+}_s}{(R^{+}_{p,i})^2}\hat{\bar{q}_s}^{+}(x,t) - \frac{45}{2(R^{+}_{p,i})^2}\hat{j}^{+}_n(x,t) \tag{4.19}$$

$$\hat{c}^{+}_{ss}(x,t) = \hat{\bar{c}_s}^{+}(x,t) + \frac{8R^{+}_{p,i}}{35}\hat{\bar{q}_s}^{+}(x,t) - \frac{R^{+}_{p,i}}{35D^{+}_s}\hat{j}^{+}_n(x,t) \tag{4.20}$$

$$\frac{\partial \hat{\phi_e}^{+}(x,t)}{\partial x} = -\frac{\hat{i}_e^{+}(x,t)}{\kappa^{+}} \tag{4.21}$$

$$\frac{\partial \hat{\phi_s}^{+}(x,t)}{\partial x} = \frac{\hat{i}_e^{+}(x,t) - I(t)}{\sigma^{+}} \tag{4.22}$$

$$\frac{\partial \hat{i}_e^{+}(x,t)}{\partial x} = \sum_{i=1}^{n} \frac{3\epsilon_{s,i}^{+}}{R_{p,i}^{+}} F \hat{j}_{n,i}^{+}(x,t) \tag{4.23}$$

$$\hat{j}_{n,i}^{+}(x,t) = \frac{\hat{i}_{0,i}^{+}(x,t)}{F}(e^{\alpha_a F \hat{\eta}_i^{+}(x,t)/RT} - e^{\alpha_c F \hat{\eta}_i^{+}(x,t)/RT}) \tag{4.24}$$

(b) Negative electrode, where $x \in [0^-, L^-]$

$$\frac{\partial}{\partial t}\hat{\bar{c}_s}^{-}(x,t) = -\frac{3}{R_{p,i}^{-}}\hat{j}_n^{-}(x,t) + \boldsymbol{\gamma}_i^{-}(V(t) - \hat{V}(t)) \tag{4.25}$$

$$\frac{\partial}{\partial t}\hat{\bar{q}_s}^{-}(x,t) = -\frac{30D_s^{-}}{(R_{p,i}^{-})^2}\hat{\bar{q}_s}^{-}(x,t) - \frac{45}{2(R_{p,i}^{-})^2}\hat{j}_n^{-}(x,t) \tag{4.26}$$

$$\hat{c}_{ss}^{-}(x,t) = \hat{\bar{c}_s}^{-}(x,t) + \frac{8R_{p,i}^{-}}{35}\hat{\bar{q}_s}^{-}(x,t) - \frac{R_{p,i}^{-}}{35D_s^{-}}\hat{j}_n^{-}(x,t) \tag{4.27}$$

$$\frac{\partial \hat{\phi_e}^{-}(x,t)}{\partial x} = -\frac{\hat{i}_e^{-}(x,t)}{\kappa^{-}} \tag{4.28}$$

$$\frac{\partial \hat{\phi_s}^{-}(x,t)}{\partial x} = \frac{\hat{i}_e^{-}(x,t) - I(t)}{\sigma^{-}} \tag{4.29}$$

$$\frac{\partial \hat{i}_e^{-}(x,t)}{\partial x} = \sum_{i=1}^{n} \frac{3\epsilon_{s,i}^{-}}{R_{p,i}^{-}} F \hat{j}_{n,i}^{-}(x,t) \tag{4.30}$$

$$\hat{j}_{n,i}^{-}(x,t) = \frac{\hat{i}_{0,i}^{-}(x,t)}{F}(e^{\alpha_a F \hat{\eta}_i^{-}(x,t)/RT} - e^{\alpha_c F \hat{\eta}_i^{-}(x,t)/RT}) \tag{4.31}$$

(c) Internal lumped temperature model of battery is given by

$$\begin{aligned}\rho^{avg} c_p \frac{d\hat{T}(t)}{dt} &= h_{cell}(T_{amb}(t) - \hat{T}(t)) + I(t)\hat{V}(t) \\ &- \sum_{(i=1)}^{n^-}[\int_{0^-}^{L^-} \frac{3\epsilon_{s,i}^{-}}{R_{p,i}^{-}} F \hat{j}_{n,i}^{-}(x,t)\Delta U_i^{-}(x,t)dx] \\ &- \sum_{(i=1)}^{n^-} +[\int_{0^+}^{L^+} \frac{3\epsilon_{s,i}^{-}}{R_{p,i}^{+}} F \hat{j}_{n,i}^{+}(x,t)\Delta U_i^{+}(x,t)dx] + \boldsymbol{\gamma}_T^{-}(T(t) - \hat{T}(t))\end{aligned} \tag{4.32}$$

Output voltage of the observer is given by,

$$\hat{V}(t) = \hat{\phi}_s^+(0^+, t) - \hat{\phi}_s^-(0^-, t) \tag{4.33}$$

4.3 Initial and Boundary Conditions of Observer

Above PDAE system initial conditions are given by,

$$\hat{\overline{c}_{s,i}}^{\pm}(x, t) = \hat{\overline{c}_{s,i,0}}^{\pm}(x) \tag{4.34}$$

$$\hat{\overline{q}_{s,i}}^{\pm}(x, t) = \hat{\overline{q}_{s,i,0}}^{\pm}(x) \tag{4.35}$$

$$\hat{T}(0) = \hat{T}_0 \tag{4.36}$$

Boundary conditions are given by,

$$\hat{\phi_e}^{+}(0^+, t) = 0, \tag{4.37}$$

$$\hat{\phi_e}^{-}(L^-, t) = \hat{\phi_e}^{+}(L^+, t) - \frac{I(t)L^{sep}}{\kappa^{sep}} \tag{4.38}$$

$$i_e^{\pm}(0^{\pm}, t) = 0 \tag{4.39}$$

$$i_e^{\pm}(L^{\pm}, t) = \pm I(t) \tag{4.40}$$

The only difference between the approximated model and the observer are the voltage error feedback in Equations 4.18 and 4.25, and temperature error feedback in Equation 4.32.

The gains γ_T, γ_i^- and γ_i^+ are the observer design parameters. γ_T^- should be tuned to large value so that estimation error in the temperature calculation is quickly removed. Design parameters, γ_i^- and γ_i^+ are very closely related to each other. The relationship between them is given by,

$$\begin{pmatrix} \gamma_i^- \\ \gamma_i^+ \end{pmatrix} = \gamma * \begin{pmatrix} \frac{1}{n^- \epsilon_{s,i}^- L^-} \\ \frac{1}{n^+ \epsilon_{s,i}^- L^+} \end{pmatrix} \tag{4.41}$$

Both gain parameters γ_T^- and $\gamma \in \mathbb{R}^+$

4.4 Simplified OCP Equation of Electrode Material

The OCP equations given in Equations 3.31 and 3.33 have higher-order terms. These higher-order terms decrease computational speed of the observer, thus limiting its application in real time. These equations can be reduced to lower order terms to increase the computational speed. Dao et al. [37] proposed simpler forms of these equations by applying non-linear curve fitting technique. The simpler forms of these equations are given by,

$$U_p = \frac{-4.875 + 5.839\ \theta_p - 1.507\ \theta_p^3 + 0.531\ \theta_p^5}{\theta_p - 1.005} \tag{4.42}$$

$$U_n = 0.15 - 0.1\ \theta_n + \frac{0.00778}{\theta_n} \tag{4.43}$$

Figure 4.2 and 4.1 show the comparison of simpler equations with the original equations.

4.5 Solving Electrochemical Model Based Observer

In this thesis work, the complex PDAEs of observer were solved using Matlab. PDAEs were discretized in both space and time domain. Finite difference numerical method was applied to solve equations. Total 193 nodes were solved along spatial domain. Time domain nodes were 1 second interval. Total 193 nodes were sufficient enough to achieve the voltage estimation error less than 0.5 %. 1 second interval of time domain was chosen keeping real time execution in mind. This interval is necessary to solve the complex PDAEs during real time.

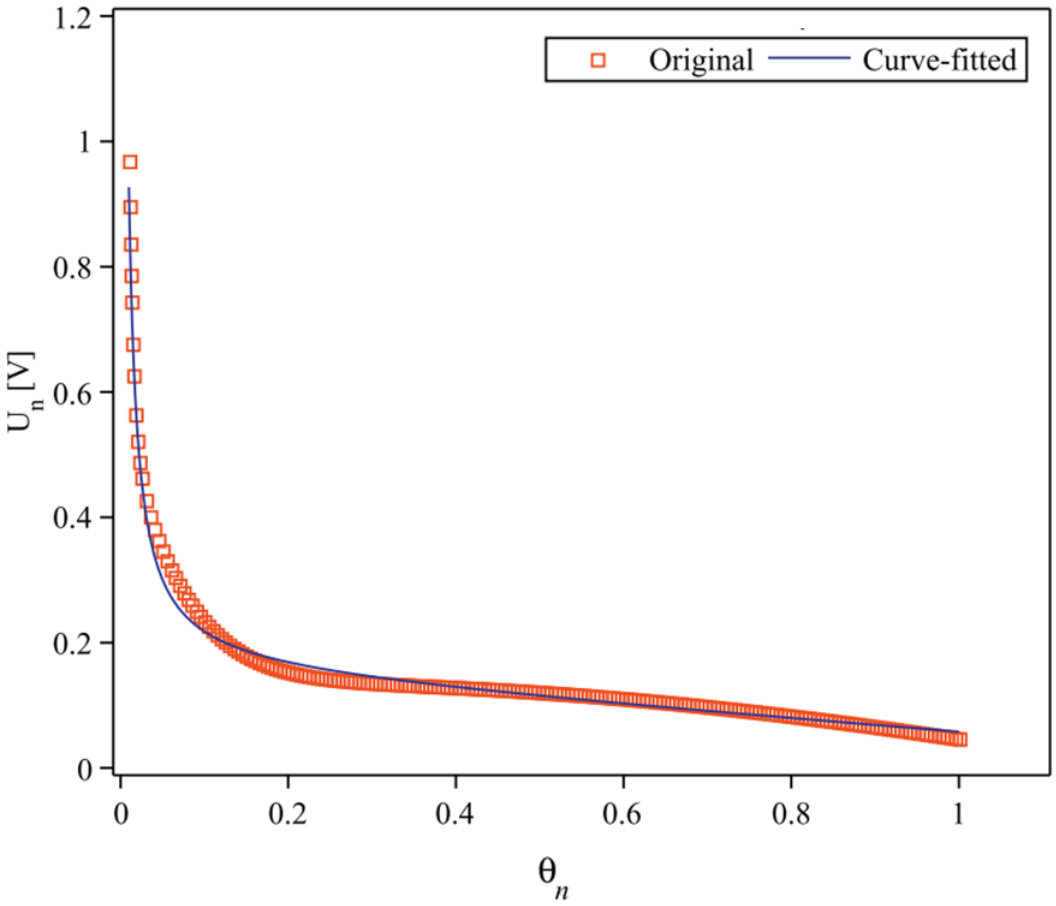

Fig. 4.1. OCP negative electrode [37]

The parameter values for $LiCoO_2$ and LiC_6 battery system which was the subject for this thesis work were chosen from [36] and are listed in Table 6.1. Observer gains were tuned by trial and error method. Figure 4.3 compares the voltage estimates from observer and plant model with different observer gains. Figure 4.3 shows that at lower observer gains(in this example gain value of 5), error was high, observer voltage was not following the plant model very closely. As and when the observer gain increases(in this example 35), observer voltage follows closely. From trial and error it's been found that observer gain of 51 was the optimum value. Figure 4.4 shows different discharge rate, 0.5C, 1C and 2C curves for full model and observer with gain of 51. As it can be seen in the Figure 4.4, estimation error decreases with the

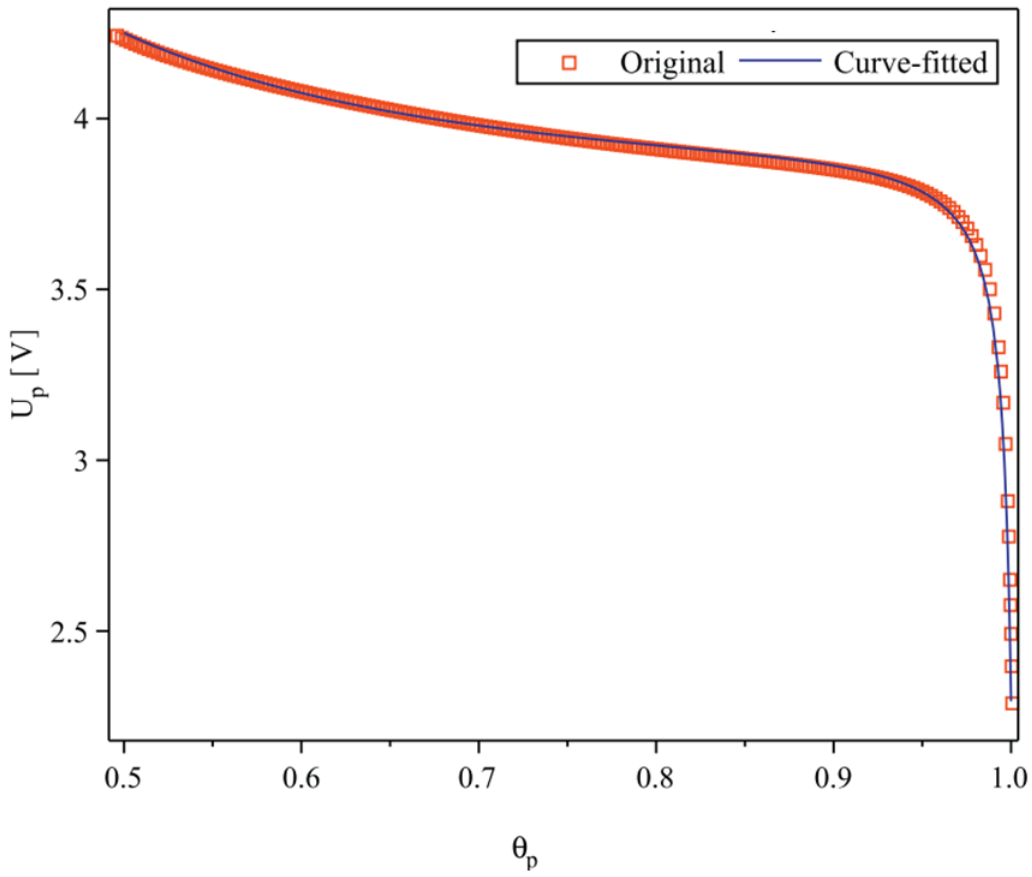

Fig. 4.2. OCP negative electrode [37]

discharge rate. Within normal operation of the cell, estimation errors were 0.025 %, 0.05 % and 0.23 % for 0.5C, 1C and 2C respectively. Similarly, Figure 4.5 shows the temperature estimate of the observer and plant model. Rate of change of temperature increased with discharge rate. Temperature was estimated very precisely with almost zero estimation error. The optimal gain for the temperature equation was 2.

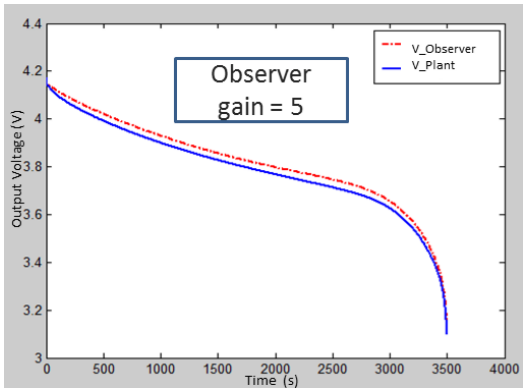

(a) Observer Gain 5

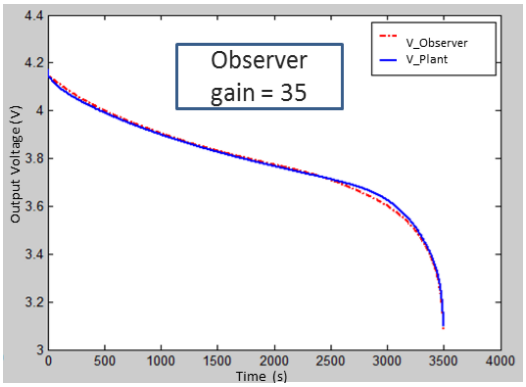

(b) Observer Gain 35

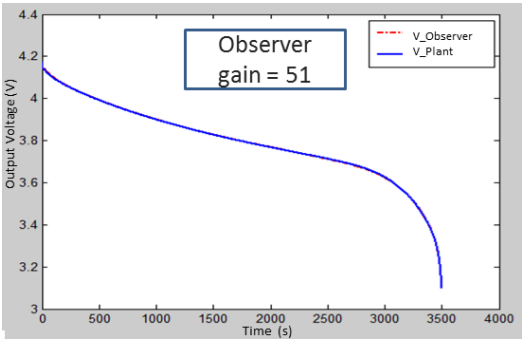

(c) Observer Gain 51

Fig. 4.3. Voltage output: Observer vs plant model at different gain values

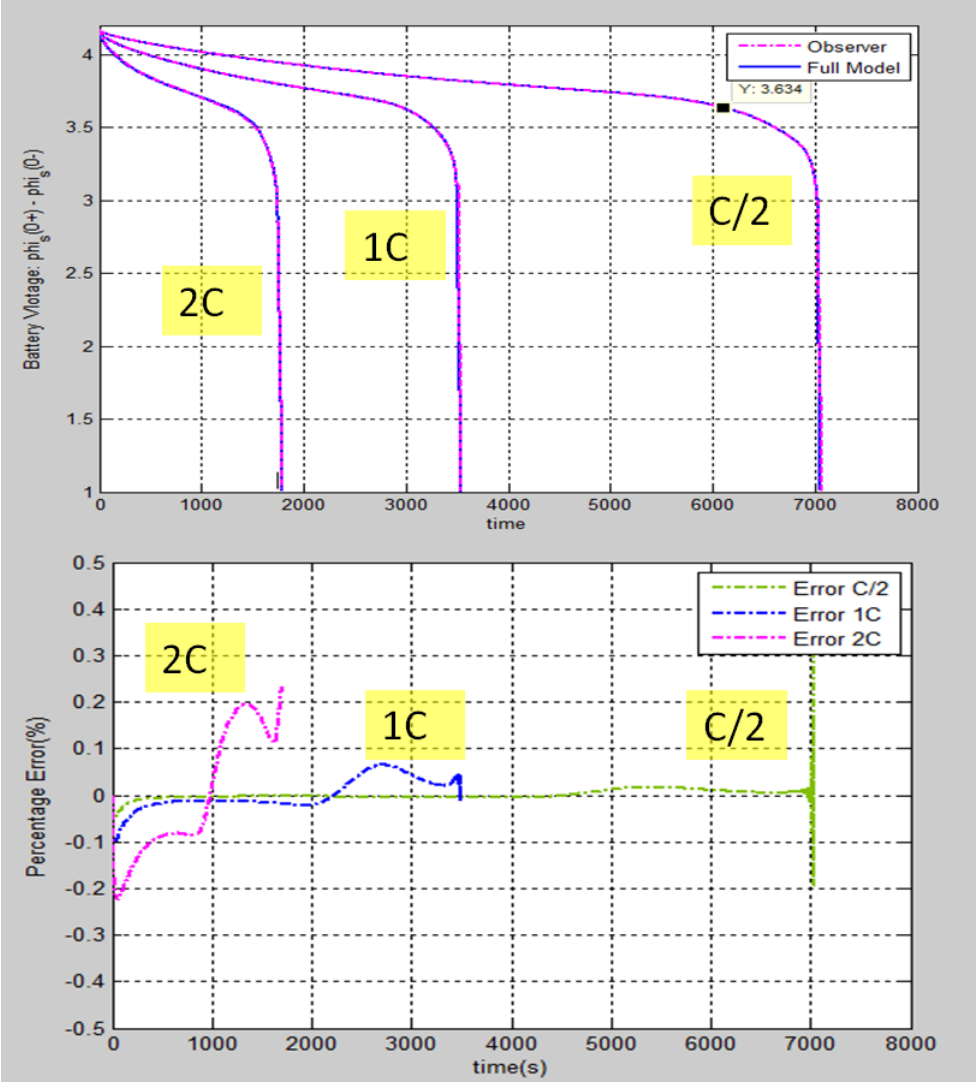

Fig. 4.4. Voltage output: Observer vs plant model at optimal gain value

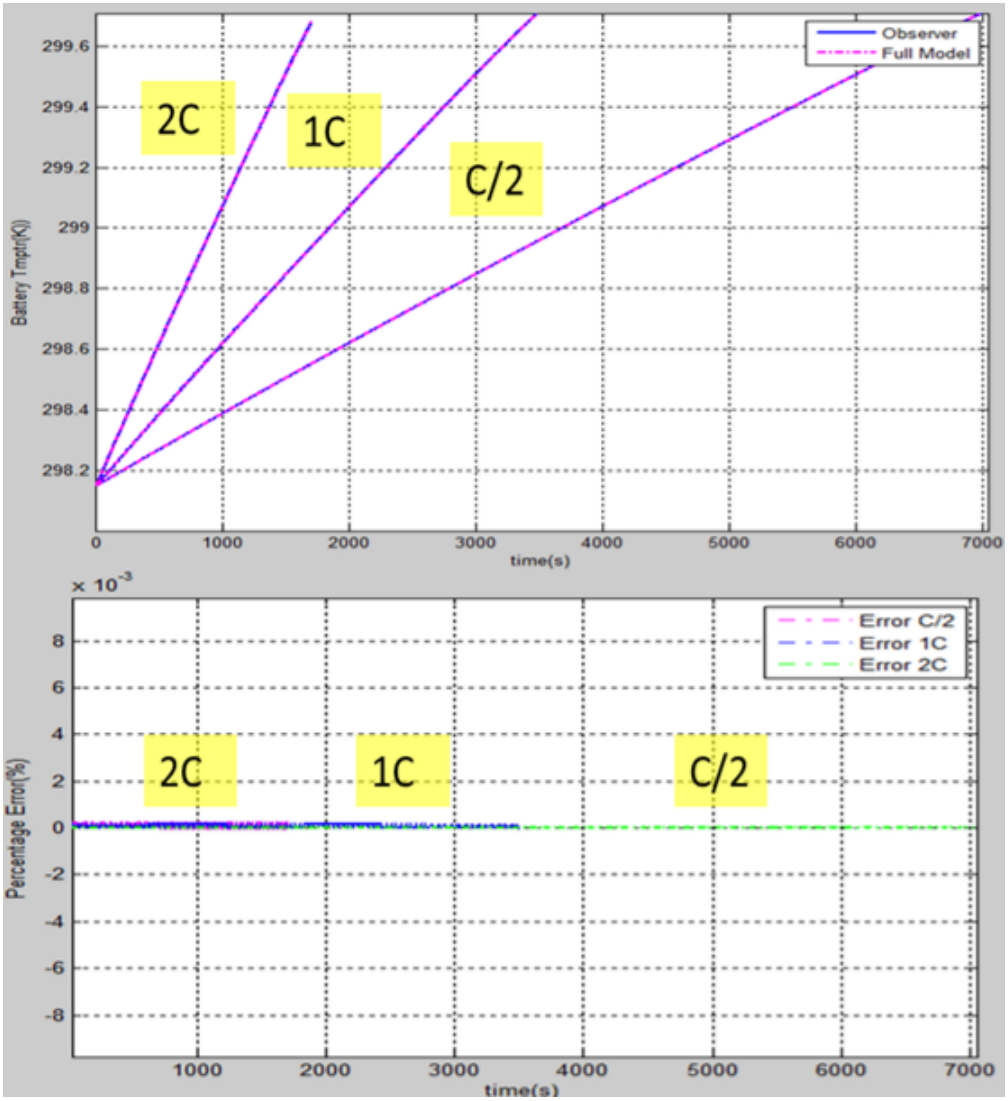

Fig. 4.5. Temperature output: Observer vs plant model at optimal gain value

5. FUZZY LOGIC BASED CONDITION DIAGNOSIS

Lithium-ion battery fault detection and diagnosis(FDD) has been systematically pursued by many researchers during last few years. The main driving force for this is the high importance of the battery in real world situations like automotive and aeronautical industry etc.

Just like any other physical system, lithium-ion batteries are designed and developed by incorporating better chemistry, protection circuitry, advanced manufacturing process etc. for increased performance and reliability. The risk of lithium-ion failures have reduced considerably with all these precautions and measures. But still a significant amount of risk leak through making them unsafe. Hence there is a need of fault detection and diagnosis system which can continuously diagnose the battery and report the fault well ahead of time. Fault diagnosis can be thought of as a simple on-off switch where in switch goes on when there is any fault detected in the system [11].

Traditional FDD methods can be classified mainly into different categories like, quantitative model based methods, qualitative model based methods and process history based methods [38]. Quantitative model based methods are based on the physics of the monitored process. Here process being monitored is represented in mathematical, functional relationship between inputs and outputs. Examples of this method are, diagnostics observers like, Kalman filter, Luenberger, physics model based etc. Qualitative methods have process input and outputs relationships represented in qualitative functions centered around the different units of process. History based methods based on historical data of the process. They do not make use of physics based information of the process. Examples of this method are, neural networks, neuro-fuzzy models, statistical methods etc. [38].

5.1 Model based FDD

In this thesis, model based FDD method has been used; as this approach captures real dynamics of lithium-ion battery enabling accurate estimation of the different states and output of the battery. This further enables the reliable early detection of the fault conditions in lithium-ion battery.

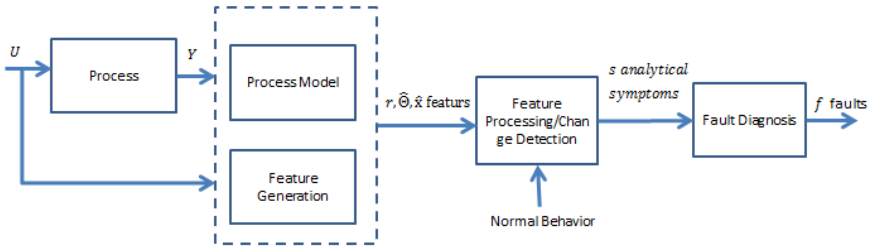

Fig. 5.1. Model based fault diagnosis block diagram [39]

Figure 5.1 shows the block diagram of basic structure of model based fault diagnosis. Process input U and output Y is fed to the process model and feature generation block to estimate different states, $\hat{x}$ or parameters, $\hat{\Theta}$ of the process model and generate residuals, r. These estimated states, parameters and generated residuals are called features. These features are further sent to feature processing and change detection block to compare them with the corresponding features generated out of normal behavior system. Comparing with normal behavior system reveals the changes of feature which are called as analytical symptoms, s; by quantifying these symptoms different faults in the system can be detected [39].

The process model used in the model based diagnosis method is the mathematical representation of the system. This mathematical representation should capture the system dynamics of the process; more essentially it should capture the system dynamics which represents faults in the process. At the same time, this process model should also be computationally inexpensive so that faults can be reliably detected in real-time applications. This is very critical in mobile applications like automotive and aeronautics industry.

There are few limitations in using the pure process model in the model based diagnostics because of modeling inaccuracies, input and output measurement noise, faulty initial conditions, unknown disturbances and system noise. These might lead to inaccurate or unstable state estimation or parameter estimation, leading to unreliable fault detection. This can be overcome by replacing the pure process model by observers [39, 40]. There are many different kinds of observers like Kalman filter, Luenberger observer, output error injection based etc. [12, 40] can be found in literature.

5.2 Simulink Design for FDD

In this thesis, a full battery model described in Chapter 3 is used for process model as it captures complete dynamics of the lithium-ion battery. Approximated lithium-ion battery model along with output error injection based observer described in Chapter 4 is used as process observer model. Matlab/Simulik model designed for the lithium-ion battery detection is shown in Figure 5.7.

Each subsystems shown in the simulink diagram corresponds to one or more functionality of the blocks shown in 5.1. 'Battery Process Model' and 'Battery Observer' subsystems represents process model and process model based observer for lithium-ion battery respectively. Feature generation subsystem takes process model and observer outputs like voltage, temperature and SOC and generates features which can be used for FDD. Generated features include,

1. Battery output voltage residual
2. Battery temperature residual
3. SOC residual
4. Battery voltage level
5. Battery temperature change

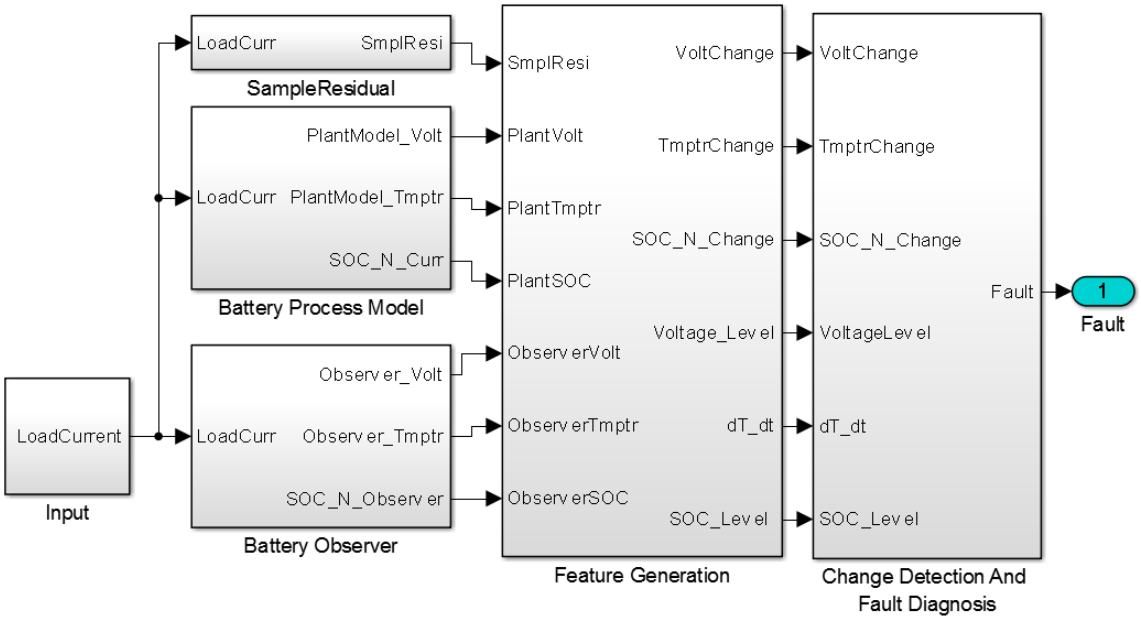

Fig. 5.2. Matlab/Simulink design for the FDD

6. Battery SOC Level

'Change detection and fault diagnosis' subsystem is fuzzy logic based. Fuzzy membership functions were designed for all features and fuzzy output fault decision signal. A strong and accurate fuzzy rule base was developed based on the analysis of faulty and healthy lithium-ion battery systems. Fuzzy rule base is shown in Table 5.1. Additionally, there exist an enable subsystem, 'FDD Enable' to enable feature generation block only during time windows when feature signatures represent true fault conditions.

5.2.1 Membership Functions(MF)

Voltage residual MF

Voltage residual is the relative error calculated in percentage(%). Figure 5.3 shows the MF for voltage residual. Three different fuzzy sets were defined namely, Z(Zero),

N(Negative) and P(Positive). Z, N and P use 'triangular', 'z' and 's' membership functions respectively. If incoming residual is close to zero then it's classified as fuzzy 'Z', if it is close to or greater than +1 then its classified as fuzzy 'P', and if it is close to or greater than -1, its classified as fuzzy 'N'. Voltage fuzzy sets range were designed based on knowledge of voltage residual for healthy and faulty battery systems.

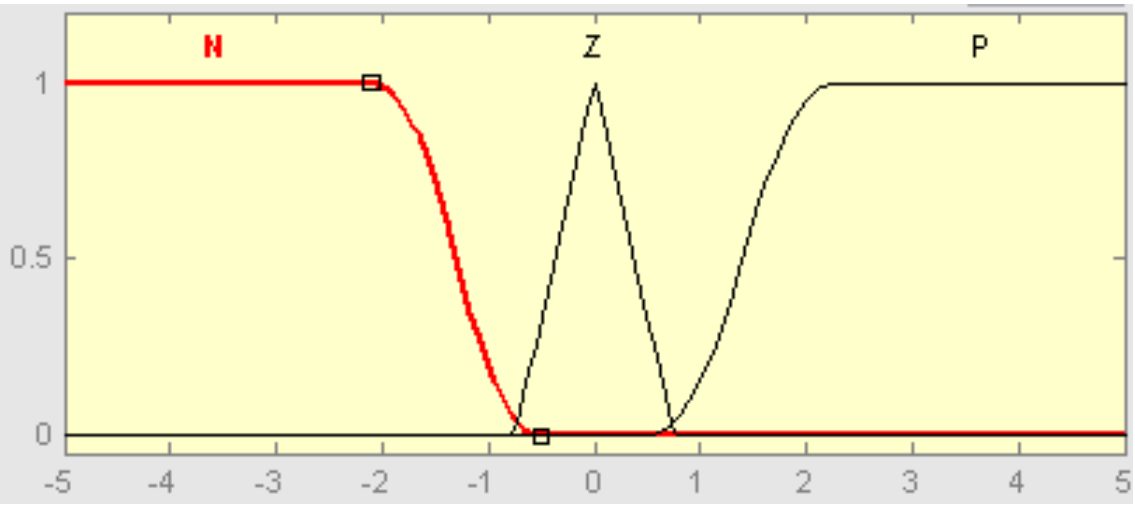

Fig. 5.3. Voltage residual fuzzy MF

Temperature residual MF

Temperature residual is the relative error calculated in percentage(%). Figure 5.4 shows the MF for temperature residual. Similar to voltage residual fuzzy sets, three different fuzzy sets were defined namely, Z(Zero), N(Negative) and P(Positive). If incoming residual is close to zero then its classified as fuzzy 'Z', if it is close to or greater than 0.2 then its classified as fuzzy 'P', and if it is close to and greater than -0.2 then its classified as fuzzy 'N'. Temperature fuzzy sets range were designed based on knowledge of temperature residual for healthy and faulty battery systems.

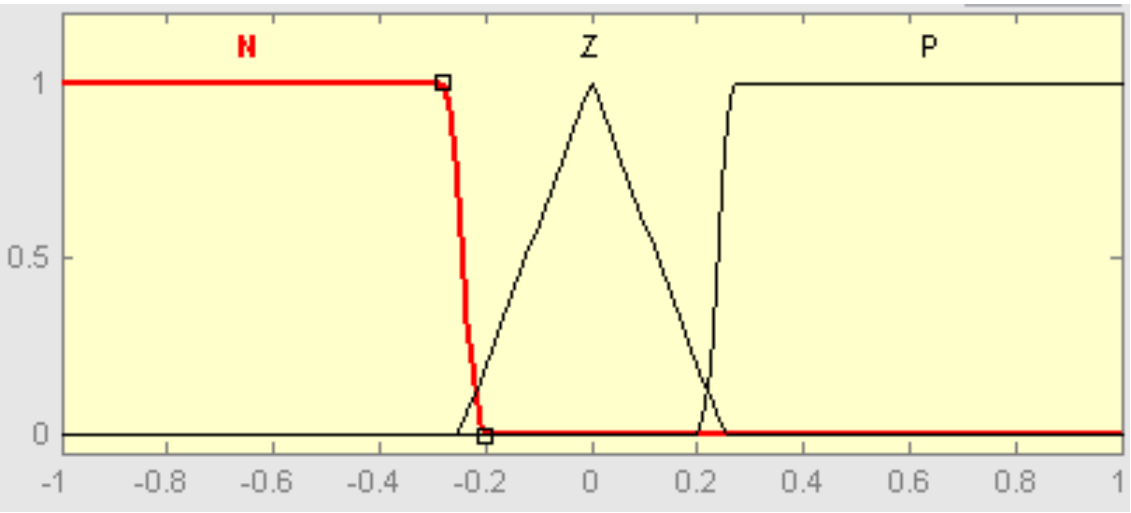

Fig. 5.4. Temperature residual fuzzy MF

SOC residual MF

SOC residual is the relative error calculated in percentage(%). Figure 5.5 shows the MF for SOC residual. Similar to voltage and temperature residuals three different fuzzy sets were defined. If incoming residual is close to zero then its classified as fuzzy 'Z', if it is close to or greater than +1 then its classified as fuzzy 'P', and if it is close to and greater than -1 then its classified as fuzzy 'N'. SOC fuzzy sets range were designed based on knowledge of SOC residual for healthy and faulty battery systems.

Battery Voltage level MF

Battery voltage level is the output voltage in volts from the battery plant model. Figure 5.6 shows the MF for battery voltage level. Three different fuzzy sets were defined, namely Nominal, Low and High. Low, Nominal and High use 's', 'trapezoidal' and 'z' membership functions respectively. If incoming signal is within 4.3 and 3.7 then its classified as fuzzy Nominal, if it is close to or less than 3.7 then its classified as fuzzy Low, and if it is close to and greater than 4.3 then its classified as fuzzy

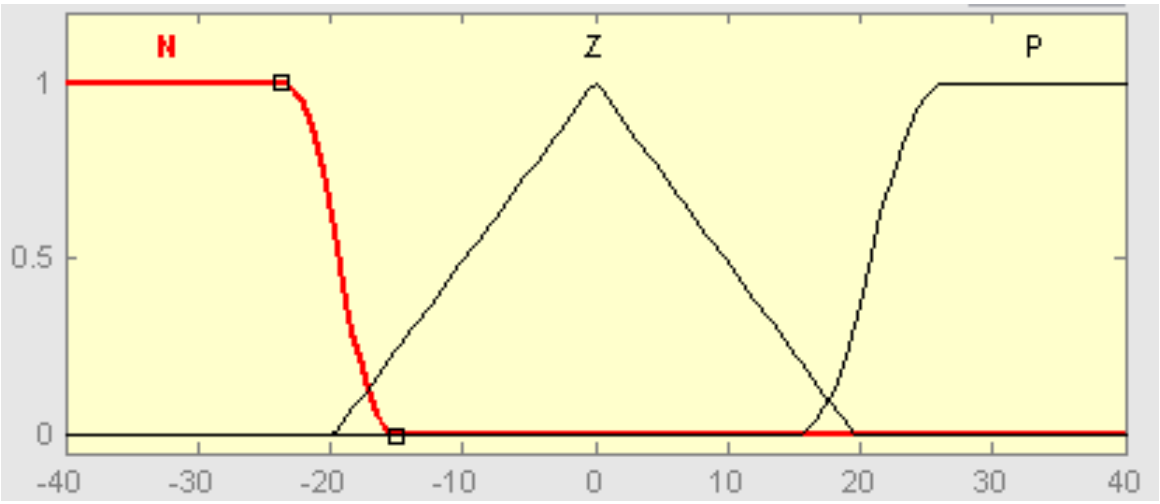

Fig. 5.5. SOC residual fuzzy membership function

High. Range of voltage level fuzzy sets were designed based on knowledge of voltage level for healthy and faulty battery system.

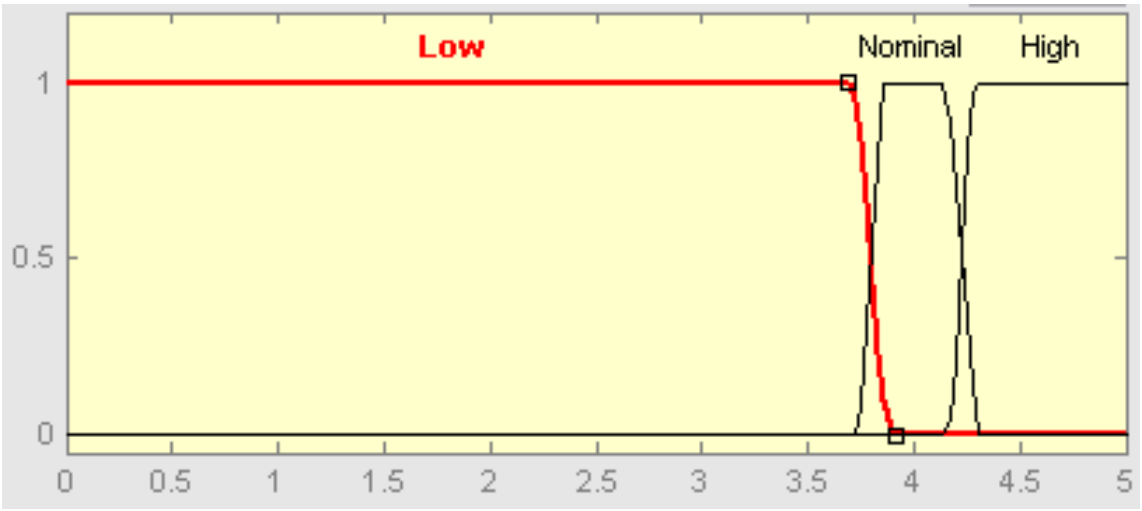

Fig. 5.6. Battery voltage level fuzzy MF

Battery Temperature change MF

Battery temperature change is the rate of change of battery temperature from plant model calculated in Kelvin per second. Figure 5.6 shows the MF for battery temperature change. Two different fuzzy sets were defined, namely Nominal and High. Nominal and High use z and s membership functions respectively. If incoming signal is greater than 0.1, its classified as fuzzy High and if it is less than 0.2 then its classified as fuzzy Nominal. Temperature change fuzzy sets range were designed based on knowledge of temperature rate change for healthy and faulty battery system.

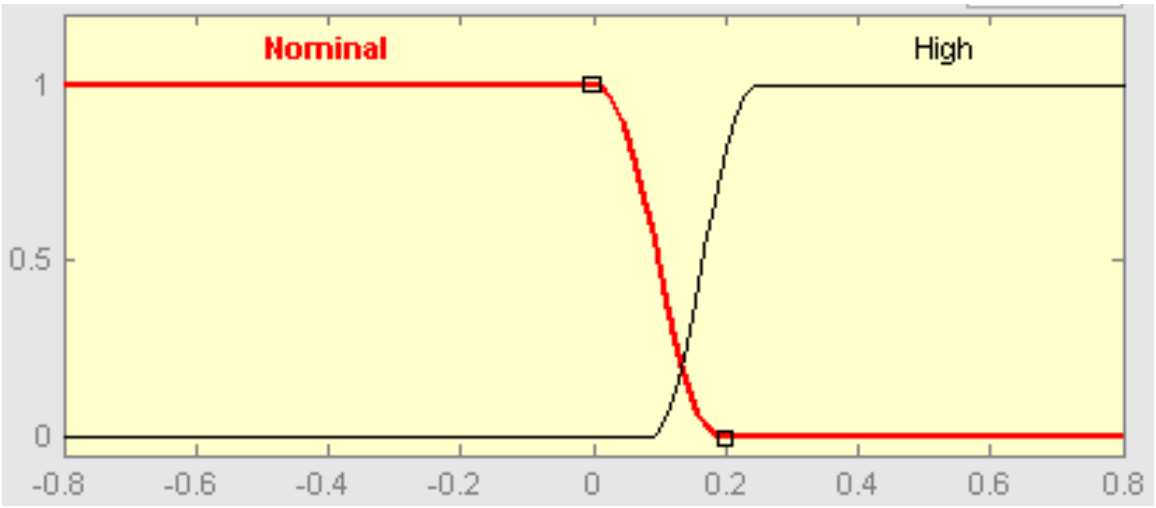

Fig. 5.7. Battery temperature change MF

Battery SOC level MF

Battery SOC level is the SOC calculated from coulomb counting approach on load current. Figure 5.8 shows the MF for battery SOC level. Three different fuzzy sets were defined, namely Nominal, Low and High. Nominal, Low and High use trapezoidal, z and s membership functions respectively. If incoming signal is between 0.9 and 0.1, its classified as fuzzy Nominal, if it is close to or less than 0.2, its

classified as fuzzy Low, and if it is close to and greater than 0.9 then its classified as fuzzy High. SOC level fuzzy sets range were designed based on knowledge of SOC level for overcharge, over-discharge and nominal battery.

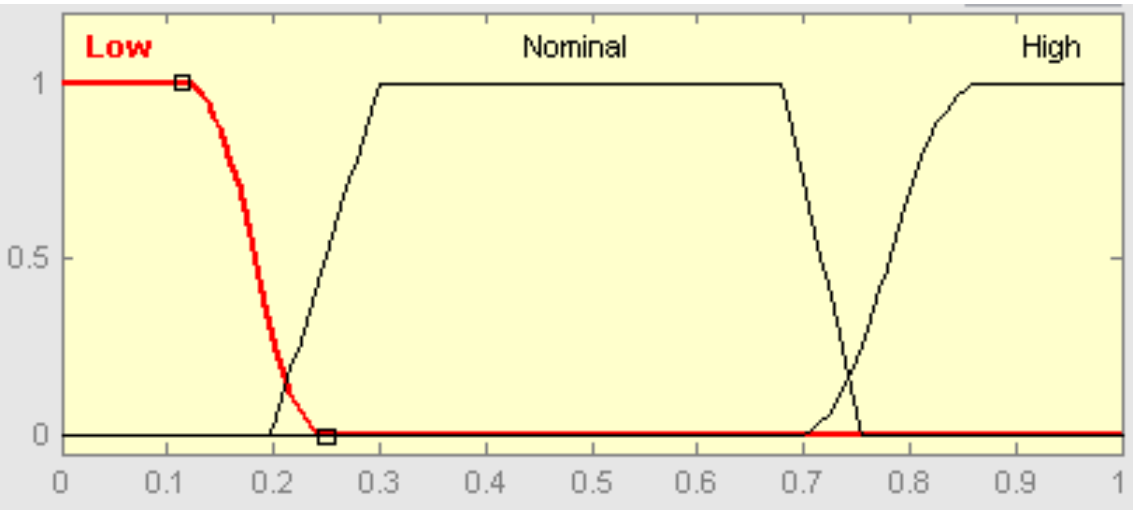

Fig. 5.8. Battery SOC level fuzzy MF

Fault decision MF

Fault decision is defuzzyfied output. Figure 5.9 shows the MF for output fault decision signal. In this MF two different fuzzy sets were defined, namely N(No Fault) and F(Fault). Both MF uses triangular membership function. -1 indicates no fault in the battery, while +1 indicates definite fault.

5.2.2 Decision Signal Generation

Fuzzy input MFs use respective 'feature' values to calculate fuzzy values. Fuzzy values decide which rules to be triggered and their degree of activation. Based on the triggered rules and their degree, decision signal gets calculated using the output MF. Centroid method was applied to derive the decision signal value from output MF.

For detailed working of the fuzzy systems used in this thesis, [41] is recommended for readers.

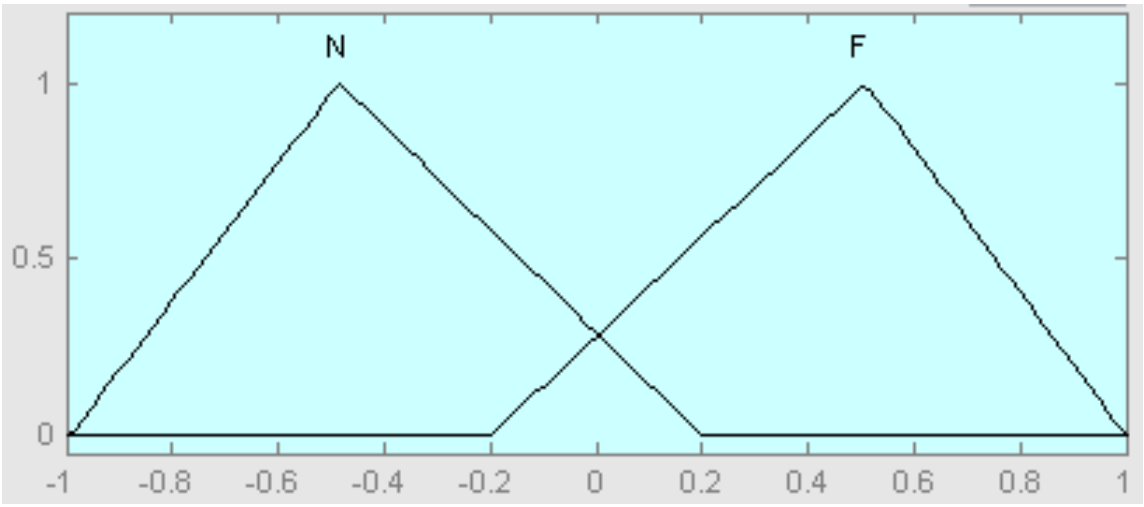

Fig. 5.9. Fault decision output MF

Table 5.1
Fuzzy rule base for the lithium-ion FDD

Voltage Residual	Temperature Residual	SOC Residual	SOC Level (Current Measurement)	Voltage Level	$\frac{dT}{dt}$ (Sensor)	Diagnostics Decision
zero	Zero	zero	X	X	X	healthy battery
positive/ negative	zero	zero	X	X	X	degraded/faulty
positive/ negative	positive/ negative	zero	low	low	positive	over discharge
positive/ negative	positive/ negative	zero	high	high	positive	over charge
positive/ negative	positive	positive/ negative	X	X	positive	internal short circuit
X	positive/ negative	X	X	X	X	faulty
X	X	positive/ negative	X	X	X	faulty

6. DESIGN OF EXPERIMENTS

6.1 Battery Chemistry and Battery Parameter Values

As mentioned in Chapter 3 and Chapter 4, a lithium-ion battery cell can be modeled using mathematical equations based on electrochemical reactions. These equations have parameters to represent different physical phenomenon like positive electrode diffusion and reaction rate constant, negative electrode diffusion and reaction rate constant, electrolyte diffusion constant, conductivity of electrode material etc. When a fault occurs in the lithium-ion battery, these electrochemical parameters, mainly, positive electrode diffusion and reaction rate constant, and negative electrode diffusion and reaction rate constant show a marked variation from their healthy battery counterparts. The primary focus of this study is the FDD of degraded/aged battery, over charge(OC), over discharge(OD), internal short circuit and any other deviation from the healthy battery operation. When considering degraded/aged battery faults the battery model parameters show a particular and distinct trend in parameter variation with battery age [42].

In this study all the dynamics of the battery is considered including temperature effects of the battery. The test subject selected for this study was $LiCoO_2$(positive electrode) and LiC_6 (negative electrode) battery system. Table 6.1 shows the parameter values for healthy battery system [36].

Ramadesigana et al. [42] have shown the effect of cycling/aging on battery parameters. For aged/degraded battery, key parameters like diffusion coefficient and reaction constant of positive electrode, diffusion coefficient and reaction constant of negative electrode and diffusion constant of electrolyte have shown significant degradation trend with aging. For OC and OD case, based on the detailed study as per [43, 44] and insight into the battery behavior during OC and OD fault conditions

Table 6.1
LiCoO2 and LiC6 system parameters used for the simulation [34]

Symbol	Unit	Positive electrode	Separator	Negative electrode
σ_i	S/m	100		100
$\epsilon_{f,i}$		0.025		0.0326
ϵ_i		0.385	0.724	0.485
B_{rugg}			4	
$D_{s,i}$	m^2/s	1×10^{-14}		3.9×10^{-14}
D	m^2/s		7.5×10^{-10}	
k_i	$Mol/(sm^2)/mol/m^3)^{1+\alpha_a,i}$	2.334^{-11}		5.0307×10^{-11}
$c_{s,i,max}$	mol/m^3	51554		30555
$c_{s,i0}$	mol/m^3	0.4955×51554		0.4955×30555
c_0	mol/m^3		1000	
R_p	m	2.0×10^{-6}		2.0×10^{-6}
l_i	$Hope.m$	80×10^{-6}	25×10^{-6}	88×10^{-6}
R_{SEI}	m^2			0.0
t_+			0.363	100
F	C/mol		96487	
R	$J/(molK)$		8.314	
T	K		298.15	

a degradation trend was presumed for these parameters. Table 6.2 shows the list of parameters which get affected and their values for the degraded/aged, OC and OD fault conditions and percentage of the degradation of these parameters as compared to healthy system. Using this data, multiple faults representing plant/process model can be formulated. Hybrid pulse power characterization(HPPC) load current cycle was applied to lithium-ion battery to demonstrate various fault conditions like degraded battery, OD and OC.

6.2 Hybrid Pulse Power Characterization Drive Cycle

HPPC was accessed from [45] and is represented in Figure 6.2. The objective of this is to demonstrate battery pulse power regeneration capabilities and discharge pulse capabilities at various SOC. The complete HPPC sequence applied on the battery is shown in Figure 6.1. The duration of load current selected for this study was 12210 seconds. HPPC drive cycle began on battery with 100 percent SOC. Between each pulse power characterization, there was a resting period to allow battery to come back to complete rest so that it can establish OCP. At the end of the HPPC cycle sequence capacity of the battery was close to zero.

Table 6.2
Healthy, Degraded, OD and OC battery parameters

Parameter	Healthy [34]	Degraded [42]	OD	OC
D_n	3.9×10^{-14}	4.8750×10^{-15}	7.8×10^{-15}	6.5×10^{-15}
D_p	1.0×10^{-14}	1.5×10^{-14}	5.0×10^{-15}	5.0×10^{-15}
k_n	5.0307×10^{-11}	6.2884×10^{-12}	1.0061×10^{-11}	8.38×10^{-12}
k_p	2.334^{-11}	2.33×10^{-11}	1.17×10^{-11}	1.17×10^{-11}
D	7.5×10^{-10}	7.5×10^{-10}	3.75×10^{-10}	$3.75 \times 10^{-}11$

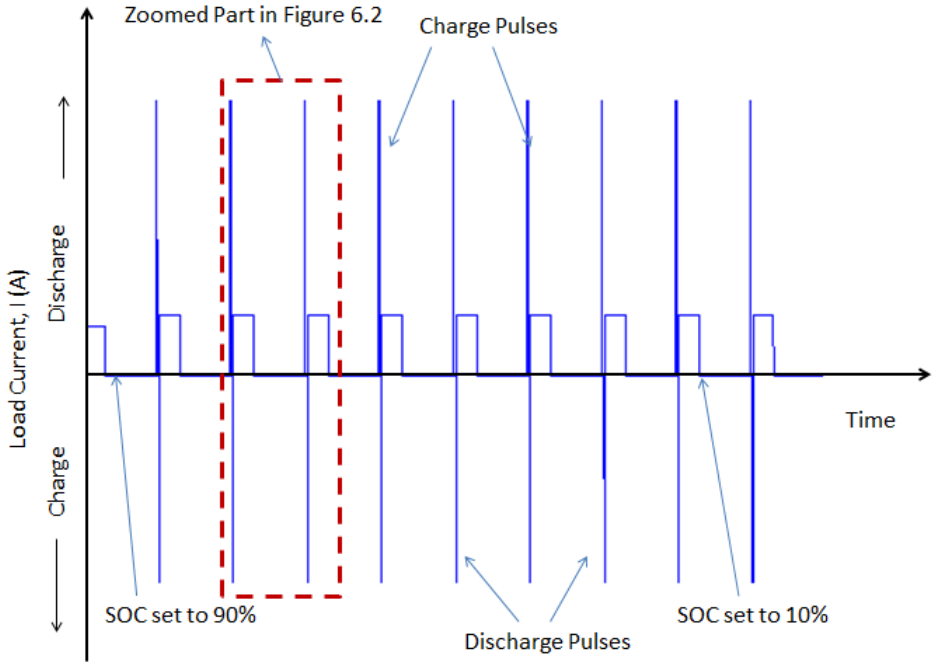

Fig. 6.1. Complete hybrid pulse power characterization Sequence

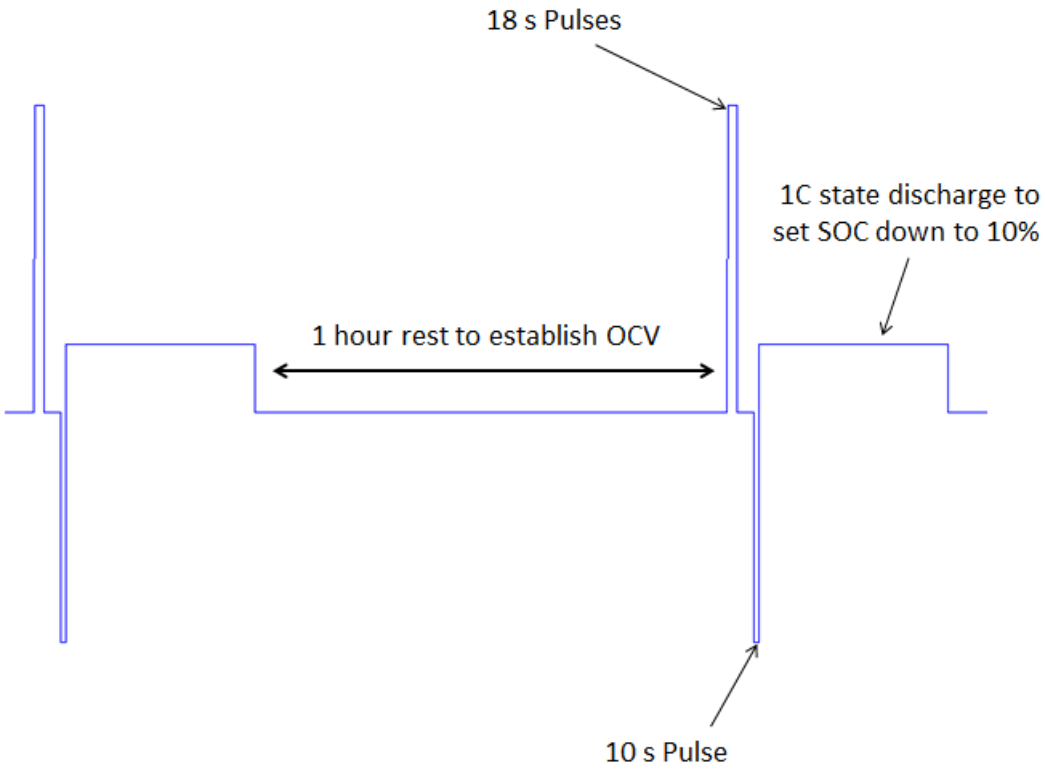

Fig. 6.2. Hybrid pulse power characterization profile

7. DIAGNOSIS PERFORMANCE EVALUATION

7.1 Fault Injection

The effectiveness of the fault diagnosis and detection was examined by injecting consecutive fault conditions and studying them. Fault conditions were injected by introducing variations in the parameters of battery model. The simulation was run for total of 12210 seconds and sample time was 1 second. Sample time was chosen keeping complex PDAEs of process observer model and their real time executions in mind. Based on today's computational capabilities, 1 second is sufficient amount of execution time to solve PDAEs. The total simulation was divided into six parts which occurred consecutively:

1. For the first 800 s healthy battery cell operation
2. For next 3500 s OC fault condition
3. For next 3500 s return to healthy battery cell operation
4. For next 3500 s degraded battery fault condition
5. For next 3500 s sample return healthy battery cell operation
6. For remaining time OD fault condition

In this setup it is assumed that only one fault can occur in the system at any given point of time. This setup helps to verify the effectiveness of the fault diagnosis and detection algorithm to de-latch itself from its earlier diagnosed conditions once operational conditions is diagnosed correctly [46].

7.2 Fault Detection

At every execution step below features were calculated:

1. Battery output voltage residual
2. Battery temperature residual
3. SOC residual
4. Battery voltage level
5. Battery temperature change
6. Battery SOC Level

The features such as voltage level, battery temperature change and SOC level were fed to fuzzy rule based fault detector at every executions step as and when they were calculated. Figure 7.1 shows these signals from plant model and observer. But, features such as voltage, temperature and SOC residuals were fed only during certain enable time window. Figure 7.2 shows these signals along with enable signal. Figure 7.3 shows zoomed version of the part highlighted in Figure 7.2. Subplot 1 of Figure 7.3 shows that, the moment when load current excitation was applied(at 1260 s, 1278 s, 1310 s and 1320 s) voltage residual value was high; it gradually decreased even though the load current remained same. This behavior was because of the output error injection and observer gain term which gave capability to the observer to converge to true value coming from the plant model. This gradually reduced the separation between faulty and healthy battery. So in order to get a good separation, residuals were sampled only during first few seconds of load current excitation. Subplot 4 in Figure 7.3 shows the 'enable' signal to sample the residuals. Fuzzy rule based fault detector ran at every simulation step to evaluate probability of fault. It calculated values between -1 and +1; +1 indicated definite fault and -1 indicated no fault or healthy behavior of the system. The resulting probabilities are shown in Figure 7.4.

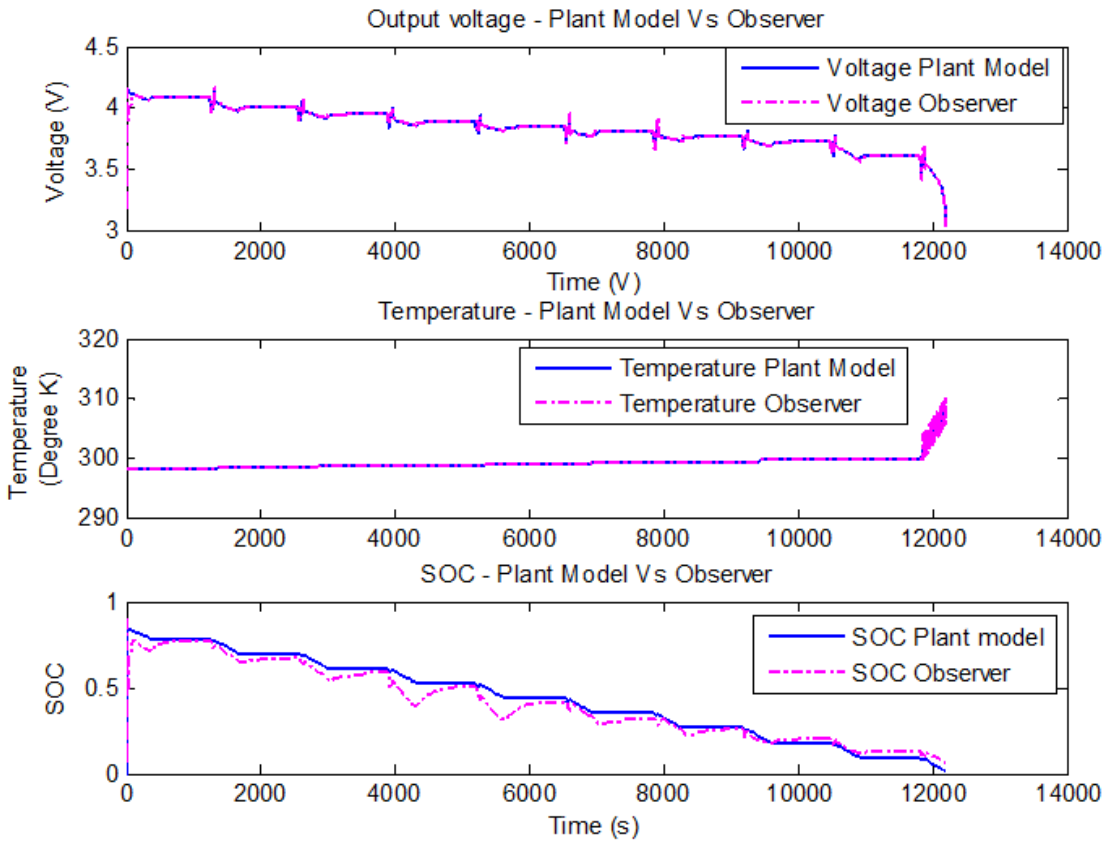

Fig. 7.1. Lithium-ion battery plant versus observer outputs

The test was run for total duration of 12210 seconds. At 1260 seconds, OC fault was indicated as probability transited from -0.5 to +0.5. At 3900 seconds, the OC probability previously at 0.5, transited to -0.5 to indicate healthy battery condition. At 6540 seconds, probability moved back to +0.5 indicating degraded battery. Further at 9180 seconds, it moved to -0.5 to indicate healthy battery. Finally at 11840 seconds, it moved to +0.5 to indicate OD fault condition. From subplot 1 of Figure 7.4 some amount of uncertainty was observed in probability. This change in the probability values was an inherent feature in fuzzy rule base. This was corrected by comparing the probability value against a threshold of 0.3. This threshold value was chosen carefully so that faults can be detected accurately without compromising on losing out any fault

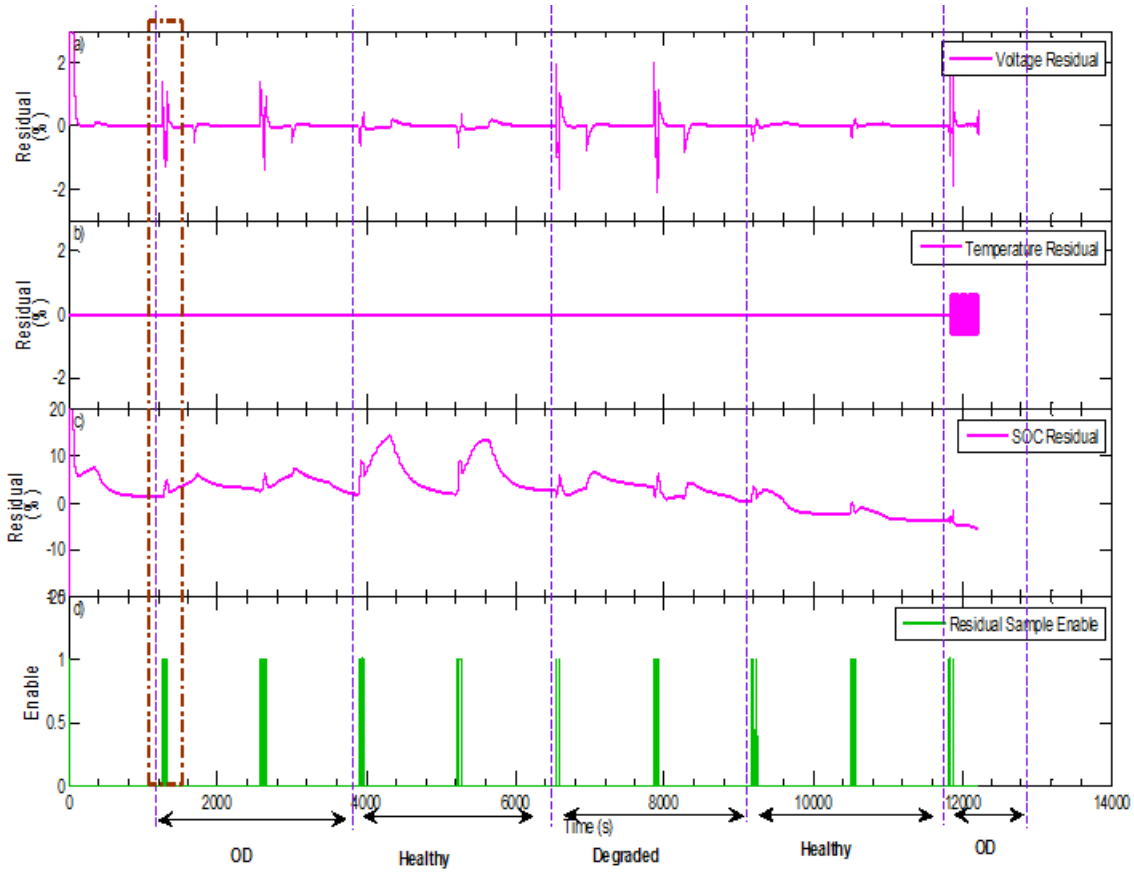

Fig. 7.2. Voltage, temperature and SOC residuals

related information. The resulting final fault decision is shown in subplot 2 of Figure 7.4. From the results it is evident that electrochemical model based observer can be successfully incorporated with the fuzzy rule based system for accurate and real time OC, degraded and OD fault detection of the lithium-ion battery energy storage device.

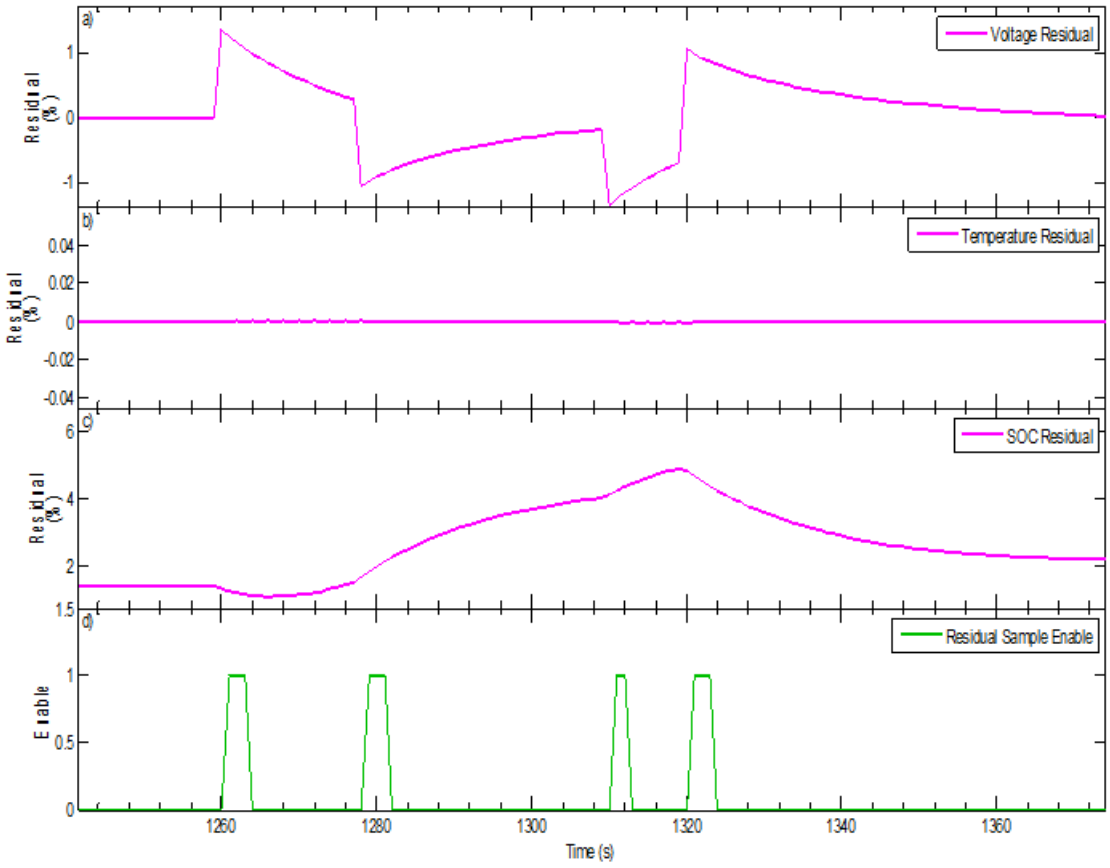

Fig. 7.3. Voltage, temperature and SOC residuals

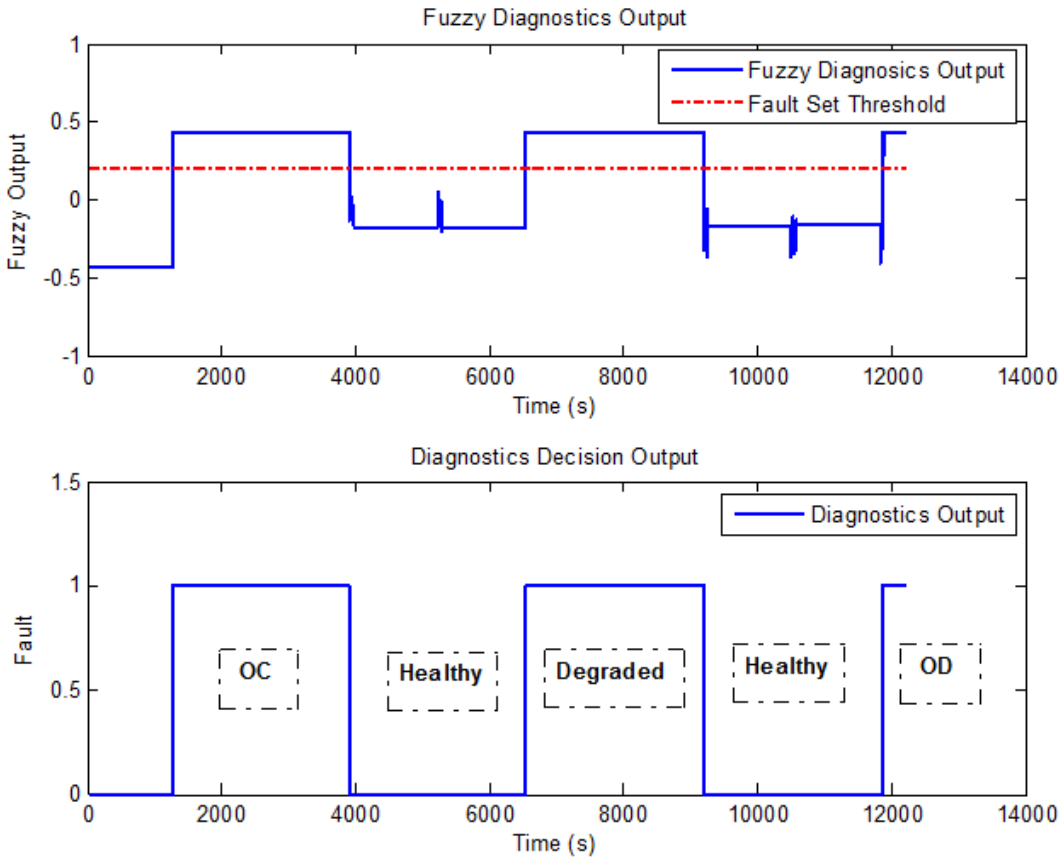

Fig. 7.4. Fuzzy output and diagnostics decision

8. CONCLUSION

8.1 Conclusion

The safety has been one of the most critical concerns for the lithium-ion batteries due to their precarious nature. For this concern in the present thesis work, an effective, practical and reliable failure detector was developed.

- Physics based electrochemical lithium-ion battery model was built to use as battery plant model. This plant model captures all the dynamics of lithium-ion battery reactions happening inside positive electrode, negative electrode and electrolyte. This model also captures temperature effects on the battery cell. This complete physics based plant model was used to verify the performance of the lithium-ion battery diagnostics.

- Approximated version of the electrochemical lithium-ion battery model along with observer capabilities was built to use as a process observer to generate features required for the model based diagnostics purpose. The approximated model reduced the computational time thus enabled design of real-time failure detector. Observer gain parameters were tuned for accurate state estimation and fault diagnosis

- Moreover, a model based failure detector was built based on fuzzy rules and electrochemical observer to detect various fault conditions like OC, degraded battery, OD, internal short circuit and any unknown fault conditions which deviates battery from its normal behavior. Model based fault detector uses load current (charging/discharging) and measured battery voltage as input to evaluate features like voltage level, SOC level and temperature change. Further, load current and measured voltage were used to estimate various states of the

battery using which features like voltage residual, temperature residual and SOC residual were calculated. These features were further used in the fuzzy rule base system to categorize them into healthy or faulty signatures, thus detecting battery failure.

- This fault detector was validated to detect fault conditions like OC, degraded battery and OD in HPPC drive cycle. Fault conditions were created by introducing the variations in parameters. Simulation results showed that the proposed method is very effective in detection of the stated faults in real-time, thus providing an effective way of diagnosing lithium-ion battery failure. This diagnostics approach captured real dynamics of the battery systems including temperature effects unlike other diagnostics methods presented in [10,11,20–22], thus giving an extra edge to detect the faults accurately.

8.2 Recommendation for Future Work

In the future, extension of the current work can be performed towards real world validation of the proposed diagnosis method.

- As the next step, fuzzy rule based fault diagnosis technique can be implemented on an on-board computer and validate on physical battery cell for different failures
- The diagnostics approach developed in this thesis is for a battery cell. It will be interesting to study how this diagnostics approach can be extended to battery module as well as pack.
- Study of battery parameter identification for various battery conditions can be carried out.
- Study of robustness of the algorithms developed can be performed.

- Incorporate developed algorithms into battery management system and study its performance.
- Design observer based on the full battery model, rather than approximated model and evaluate its real-time application capability.

LIST OF REFERENCES

LIST OF REFERENCES

[1] R. Wang, *Lithium ion battery failure detection using temperature difference between internal point and surface*. Indianapolis, Indiana: Purdue University, 2011.

[2] N. Chaturvedi, R. Klein, J. Christensen, J. Ahmed, and A. Kojic, "Modeling, estimation, and control challenges for lithium-ion batteries," in *American Control Conference (ACC), 2010*, pp. 1997–2002, June 2010.

[3] M. F. S. S. M. Mahdi Alavi and M. Saif, *Diagnostics in Lithium-Ion Batteries: Challenging Issues and Recent Achievements*. Springer Berlin Heidelberg, 2013.

[4] S. Levy and P. Bro, *Battery hazards and accident prevention*. Springer-Verlag US: Springer US, 1994.

[5] *Information on batteries, lithium-ion battery, rechargeable, Li-ion, NiMH, Ready2Use, NiCd, lithium polymer batteries, the memory effect*. 2014. [online] 2014, `http://www.digimax.rs/obaterijama.php/` (Accessed: 28 April 2014).

[6] D. Deng, M. G. Kim, J. Y. Lee, and J. Cho, "Green energy storage materials: Nanostructured tio2 and sn-based anodes for lithium-ion batteries," *Energy Environ. Sci.*, vol. 2, pp. 818–837, 2009.

[7] H. Choii, *A study of the mechanism of the electrochemical reaction of lithium with coo by two-dimensional soft x-ray absorption spectroscopy (2d xas), 2d raman, and 2d heterospectral xas- raman correlation analysis*, vol. 107. J. Phys. Chem. B, 2003.

[8] G. G. Amatucci, J. M. Tarascon, and L. C. Klein, "Coo2, the end member of the li x coo2 solid solution," *Journal of The Electrochemical Society*, vol. 143, no. 3, pp. 1114–1123, 1996.

[9] S. Alavi, M. Samadi, and M. Saif, "Diagnostics in lithium-ion batteries: Challenging issues and recent achievements," in *Integration of Practice-Oriented Knowledge Technology: Trends and Prospectives* (M. Fathi, ed.), pp. 277–291, Springer Berlin Heidelberg, 2013.

[10] W. Chen, W.-T. Chen, M. Saif, M.-F. Li, and H. Wu, "Simultaneous fault isolation and estimation of lithium-ion batteries via synthesized design of luenberger and learning observers," *Control Systems Technology, IEEE Transactions on*, vol. 22, pp. 290–298, Jan 2014.

[11] A. Singh, A. Izadian, and S. Anwar, "Fault diagnosis of li-ion batteries using multiple-model adaptive estimation," in *Industrial Electronics Society, IECON 2013 - 39th Annual Conference of the IEEE*, pp. 3524–3529, Nov 2013.

[12] R. Klein, N. Chaturvedi, J. Christensen, J. Ahmed, R. Findeisen, and A. Kojic, "Electrochemical model based observer design for a lithium-ion battery," *Control Systems Technology, IEEE Transactions on*, vol. 21, pp. 289–301, March 2013.

[13] K. Smith, "Electrochemical control of lithium-ion batteries [applications of control]," *Control Systems, IEEE*, vol. 30, pp. 18–25, April 2010.

[14] K. Smith, C. Rahn, and C.-Y. Wang, "Model-based electrochemical estimation and constraint management for pulse operation of lithium ion batteries," *Control Systems Technology, IEEE Transactions on*, vol. 18, pp. 654–663, May 2010.

[15] S. Santhanagopalan and R. E. White, "Online estimation of the state of charge of a lithium ion cell," *ECS Transactions*, vol. 3, no. 27, pp. 191–208, 2007.

[16] D. Di Domenico, A. Stefanopoulou, and G. Fiengo, "Lithium-ion battery state of charge and critical surface charge estimation using an electrochemical model-based extended kalman filter," *Journal of Dynamic Systems, Measurement, and Control*, vol. 132, no. 6, p. 061302, 2010.

[17] B. Saha, K. Goebel, S. Poll, and J. Christophersen, "An integrated approach to battery health monitoring using bayesian regression and state estimation," in *Autotestcon, 2007 IEEE*, pp. 646–653, Sept 2007.

[18] B. Saha and K. Goebel, "Uncertainty management for diagnostics and prognostics of batteries using bayesian techniques," in *Aerospace Conference, 2008 IEEE*, pp. 1–8, March 2008.

[19] J. Liu, A. Saxena, K. Goebel, B. Saha, and W. Wang, "An adaptive recurrent neural network for remaining useful life prediction of lithium-ion batteries," *Annual Conference of the Prognostics and Health Management Society*, 2010.

[20] A. Nuhic, T. Terzimehic, T. Soczka-Guth, M. Buchholz, and K. Dietmayer, "Health diagnosis and remaining useful life prognostics of lithium-ion batteries using data-driven methods," *Journal of Power Sources*, vol. 239, no. 0, pp. 680 – 688, 2013.

[21] D. Wang, Q. Miao, and M. Pecht, "Prognostics of lithium-ion batteries based on relevance vectors and a conditional three-parameter capacity degradation model," *Journal of Power Sources*, vol. 239, no. 0, pp. 253 – 264, 2013.

[22] J. Kozlowski, "Electrochemical cell prognostics using online impedance measurements and model-based data fusion techniques," in *Aerospace Conference, 2003. Proceedings. 2003 IEEE*, vol. 7, pp. 3257–3270, March 2003.

[23] D. Solomatine, L. See, and R. Abrahart, eds., *Practical Hydroinformatics Computational Intelligence and Technological Developments in Water Applications*, vol. 8 of *Water Science and Technology Library*, Chap. 2, pp. 17–32. Springer, 2008.

[24] J. Xiong, H. Banvait, L. Li, Y. Chen, J. Xie, Y. Liu, M. Wu, and J. Chen, "Failure detection for over-discharged li-ion batteries," in *Electric Vehicle Conference (IEVC), 2012 IEEE International*, pp. 1–5, March 2012.

[25] M. Roscher, J. Assfalg, and O. Bohlen, "Detection of utilizable capacity deterioration in battery systems," *Vehicular Technology, IEEE Transactions on*, vol. 60, pp. 98–103, Jan 2011.

[26] O. Tremblay, L.-A. Dessaint, and A.-I. Dekkiche, "A generic battery model for the dynamic simulation of hybrid electric vehicles," in *Vehicle Power and Propulsion Conference, 2007. VPPC 2007. IEEE*, pp. 284–289, Sept 2007.

[27] H. He, R. Xiong, and J. Fan, "Evaluation of lithium-ion battery equivalent circuit models for state of charge estimation by an experimental approach," *Energies*, vol. 4, no. 4, pp. 582–598, 2011.

[28] J. Newman and W. Tiedemann, "Porous-electrode theory with battery applications," *AIChE Journal*, vol. 21, no. 1, pp. 25–41, 1975.

[29] M. Doyle, T. F. Fuller, and J. Newman, "Modeling of galvanostatic charge and discharge of the lithium/polymer/insertion cell," *Journal of The Electrochemical Society*, vol. 140, no. 6, pp. 1526–1533, 1993.

[30] T. F. Fuller, M. Doyle, and J. Newman, "Simulation and optimization of the dual lithium ion insertion cell," *Journal of The Electrochemical Society*, vol. 141, no. 1, pp. 1–10, 1994.

[31] I. J. Ong and J. Newman, "Doublelayer capacitance in a dual lithium ion insertion cell," *Journal of The Electrochemical Society*, vol. 146, no. 12, pp. 4360–4365, 1999.

[32] A. J. Bard and L. R. Faulkner, *Electrochemical Methods: Fundamentals and Applications*. John Wiley & Sons, Inc, Dec. 2001.

[33] P. Albertus, J. Christensen, and J. S. Newman, "Experiment on a modeling of positive electrodes with multiple active materials for lithium-ion batteries," *Electrochemical Society*, vol. 156, p. A606, 2009.

[34] V. R. Subramanian, V. D. Diwakar, and D. Tapriyal, "Efficient macro-micro scale coupled modeling of batteries," *Journal of The Electrochemical Society*, vol. 152, no. 10, pp. A2002–A2008, 2005.

[35] L. O. Valen and J. N. Reimers, "Transport properties of lipf6-based li-ion battery electrolytes," *Journal of The Electrochemical Society*, vol. 152, no. 5, pp. A882–A891, 2005.

[36] V. R. Subramanian, V. Boovaragavan, and V. D. Diwakar, "Toward real-time simulation of physics based lithium-ion battery models," *Electrochemical and Solid-State Letters*, vol. 10, no. 11, pp. A255–A260, 2007.

[37] T.-S. Dao, C. P. Vyasarayani, and J. McPhee, "Simplification and order reduction of lithium-ion battery model based on porous-electrode theory," *Journal of Power Sources*, vol. 198, no. 0, pp. 329 – 337, 2012.

[38] A. Lemos, W. Caminhas, and F. Gomide, "Adaptive fault detection and diagnosis using an evolving fuzzy classifier," *Information Sciences*, vol. 220, no. 0, pp. 64 – 85, 2013. Online Fuzzy Machine Learning and Data Mining.

[39] R. Isermann, "Model-based fault-detection and diagnosis status and applications," *Annual Reviews in Control*, vol. 29, no. 1, pp. 71 – 85, 2005.

[40] S. X. Ding, *Model-based Fault Diagnosis Techniques: Design Schemes, Algorithms, and Tools*. Springer Publishing Company, Incorporated, 1st ed., 2008.

[41] *Fuzzy Logic Toolbox Users Guide*. The MathWorks, Inc, 2014. [online], `http://www.mathworks.com/help/pdf_doc/fuzzy/fuzzy.pdf/` (Accessed: 28 April 2014).

[42] V. Ramadesigan, V. Boovaragavan, M. Arabandi, K. Chen, H. Tsukamoto, R. Braatz, and V. Subramanian, "Parameter estimation and capacity fade analysis of lithium-ion batteries using first-principles-based efficient reformulated models," *ECS Transactions*, vol. 19, no. 16, pp. 11–19, 2009.

[43] T. Ohsaki, T. Kishi, T. Kuboki, N. Takami, N. Shimura, Y. Sato, M. Sekino, and A. Satoh, "Overcharge reaction of lithium-ion batteries," *Journal of Power Sources*, vol. 146, no. 12, pp. 97 – 100, 2005. Selected papers pressented at the 12th International Meeting on Lithium Batteries 12th International Meeting on Lithium Batteries.

[44] H.-F. LI, J.-K. GAO, and S.-L. ZHANG, "Effect of overdischarge on swelling and recharge performance of lithium ion cells," *Chinese Journal of Chemistry*, vol. 26, no. 9, pp. 1585–1588, 2008.

[45] J. Barnes, V. Battaglia, and et al. Jeff Belt, *PNGV Battery Test Manual*. Idaho National Engineering and Environmental Laboratory, rev. 3 ed., 2001. See also URL `http://avt.inel.gov/battery/`.

[46] A. Izadian and P. Famouri, "Fault diagnosis of mems lateral comb resonators using multiple-model adaptive estimators," *Control Systems Technology, IEEE Transactions on*, vol. 18, pp. 1233–1240, Sept 2010.